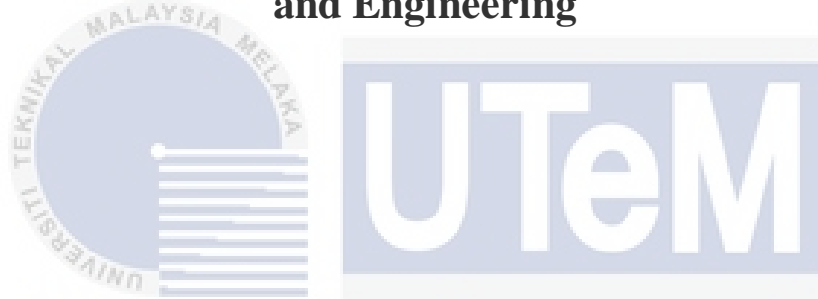




**Faculty of Electronics and Computer Technology  
and Engineering**



**DESIGN OF A MILLIMETER WAVE REFLECTARRAY ANTENNA  
FOR 5G COMMUNICATION SYSTEMS**

**LOGHAPIRITHAN A/L LOGANATHAN**

**Bachelor of Electronics Engineering Technology (Telecommunications) with Honours**

**2024**

**DESIGN OF A MILLIMETER WAVE REFLECTARRAY ANTENNA FOR 5G  
COMMUNICATION SYSTEMS**

**LOGHAPIRITHAN A/L LOGANATHAN**

**A project report submitted  
in partial fulfillment of the requirements for the degree of  
Bachelor of Electronics Engineering Technology (Telecommunications) with Honours**



**Faculty of Electronics and Computer Technology and Engineering**

**UNIVERSITI TEKNIKAL MALAYSIA MELAKA**

**UNIVERSITI TEKNIKAL MALAYSIA MELAKA**

**2024**

## DECLARATION

I declare that this project report entitled “DESIGN OF A MILLIMETER WAVE REFLECTARRAY ANTENNA FOR 5G COMMUNICATION SYSTEMS” is the result of my own research except as cited in the references. The project report has not been accepted for any degree and is not concurrently submitted in candidature of any other degree .

Signature

:



Student Name

:

Loghapirithan A/L Loganathan

Date

:

13/02/2024



## APPROVAL

I hereby declare that I have checked this project report and in my opinion, this project report is adequate in terms of scope and quality for the award of the degree of Bachelor of Electronics Engineering Technology (Telecommunications) with Honours.

Signature

: 

**DR. MUHAMMAD INAM ABBASI**

Senior Lecturer  
Department of Electronics And Computer Engineering Technology  
Faculty Of Electronics and Computer Technology and Engineering  
University Teknikal Malaysia Melaka

Supervisor Name

: DR. MUHAMMAD INAM ABBASI

Date

: 13/02/2024

اونيورسيتي تيكنيكل مليسيا ملاك

UNIVERSITI TEKNIKAL MALAYSIA MELAKA

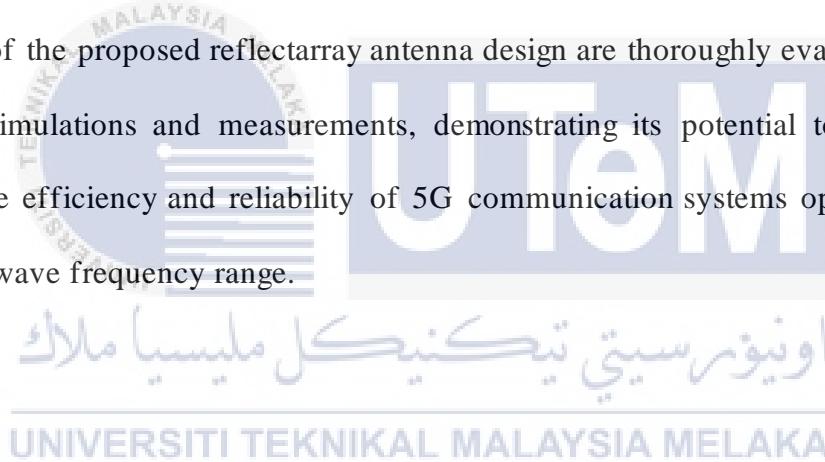
## DEDICATION

*This thesis is dedicated to my parents, whose love and support have been my driving force. To my project supervisor, Dr. Muhammad Inam Abbasi, your mentorship and guidance have shaped this research. A special thanks to lab assistant, whose diligence and collaboration significantly contributed to the project's success. This achievement is a tribute to the enduring influence of my parents and the invaluable contributions of Dr. Muhammad Inam Abbasi.*



## ABSTRACT

This research presents a novel design of a reflectarray antenna optimized for 5G communication systems, specifically operating at a frequency of 28 GHz. The reflectarray antenna structure incorporates unit cells to facilitate efficient operation in the 28 GHz frequency band. With an array of individually controlled elements, the antenna offers precise phase manipulation, enabling advanced beamforming and beam-steering capabilities. The primary objective of this design is to achieve wideband performance, high-gain characteristics, and enhanced coverage for 5G applications at 28 GHz. The performance and feasibility of the proposed reflectarray antenna design are thoroughly evaluated through extensive simulations and measurements, demonstrating its potential to significantly improve the efficiency and reliability of 5G communication systems operating in the millimeter-wave frequency range.



## ***ABSTRAK***

Penyelidikan ini membentangkan reka bentuk baru antena pemantul cahaya yang mampu beroperasi pada frekuensi resonan, khususnya pada 28 GHz, untuk memenuhi keperluan sistem komunikasi 5G. Struktur antena reflectarray menggabungkan sel unit resonan, memudahkan operasi yang cekap pada frekuensi tersebut. Dengan pelbagai elemen dikawal secara individu, antena menawarkan manipulasi fasa yang tepat, membolehkan pembentukan pancaran termaju dan keupayaan stereng pancaran. Objektif utama reka bentuk ini adalah untuk mencapai prestasi jalur lebar, ciri keuntungan tinggi, dan liputan yang dipertingkatkan untuk aplikasi 5G. Prestasi dan kebolehlaksanaan reka bentuk antena reflectarray yang dicadangkan dinilai secara menyeluruh melalui simulasi dan pengukuran yang meluas, menunjukkan potensinya untuk meningkatkan kecekapan dan kebolehpercayaan sistem komunikasi 5G yang beroperasi dengan ketara dalam julat frekuensi gelombang milimeter.

UNIVERSITI TEKNIKAL MALAYSIA MELAKA

## ACKNOWLEDGEMENTS

I would like to begin by expressing my heartfelt gratitude to my supervisor, DR Muhammad Inam Abbasi, for their invaluable guidance, wisdom, and unwavering support throughout this project. Their patience and expertise have been instrumental in shaping the success of my study.

I am also deeply thankful to my parents, parents-in-law, and beloved family members for their constant love, encouragement, and prayers during my entire period of study. Their unwavering support has been a constant source of motivation for me, and I am truly grateful for their presence in my life.

Furthermore, I would like to extend a special thank you to my dear friends who have stood by me with unwavering encouragement and cooperation throughout this journey. Their support has been indispensable, and I am truly grateful for the strong bond we share.

I am also indebted to all those who have provided me with valuable suggestions and comments during my research. Your input has greatly contributed to the development of this study, and I sincerely appreciate your insights.

Finally, I would like to express my heartfelt appreciation to all individuals who have played a significant role in the completion of this FYP report. Although I regret not being able to personally mention each one of you, please know that your contributions have not gone unnoticed. Thank you all for your support, and I am sincerely grateful for your presence in my academic journey.

## TABLE OF CONTENTS

	<b>PAGE</b>
<b>DECLARATION</b>	
<b>APPROVAL</b>	
<b>DEDICATIONS</b>	
<b>ABSTRACT</b>	<b>i</b>
<b>ABSTRAK</b>	<b>ii</b>
<b>ACKNOWLEDGEMENTS</b>	<b>iii</b>
<b>TABLE OF CONTENTS</b>	<b>iv</b>
<b>LIST OF TABLES</b>	<b>vi</b>
<b>LIST OF FIGURES</b>	<b>vii</b>
<b>LIST OF APPENDICES</b>	<b>xi</b>
<b>CHAPTER 1 INTRODUCTION</b>	<b>1</b>
1.1 Background	1
1.2 Global and Societal Issues	2
1.3 Challenges	3
1.4 Problem Statement	4
1.5 Project Objective	5
1.6 Scope and Limitations of Project	5
1.7 Summary	7
<b>CHAPTER 2 LITERATURE REVIEW</b>	<b>8</b>
2.1 Introduction	8
2.2 5G Communications Systems	8
2.3 Reflectarray for 5G communications	9
2.3.1 Dual-Band Dual-Linear Polarization Reflectarray for mmWaves/5G Applications	9
2.3.2 Design of compact millimeter wave massive MIMO dual-band (28/38 GHz) antenna array for future 5G communication systems	11
2.3.3 Evolutionary design of a dual band E-shaped patch antenna for 5G mobile communications	12
2.3.4 Design of a Wideband Reflectarray Element for Dual Band Operation in 5G Communications	14
2.3.5 A singly fed dual-band microstrip antenna for microwave and millimeter-wave applications in 5G wireless communication	15
2.3.6 Dual-Band Reflectarray Antennas Using Integrated Resonant and Non-Resonant Natures of Metallic Waveguide Elements at Millimeter Wave Frequencies	17

2.3.7	Wideband Millimeter-Wave Microstrip Reflectarray Using Dual-Resonance Unit Cells	19
2.3.8	Polarization Diversity and Adaptive Beamsteering for 5G Reflectarrays: A Review	20
2.3.9	Dual-band microstrip patch antenna array for 5G mobile communication	22
2.3.10	Dual-Band (28,38) GHz Coupled Quarter-Mode Substrate-Integrated Waveguide Antenna Array for Next-Generation Wireless Systems	23
2.4	Table of Literature Review	24
2.5	Summary	29
<b>CHAPTER 3 METHODOLOGY</b>		<b>30</b>
3.1	Introduction	30
3.2	Sustainability Development	31
3.3	Flowchart of this project	32
3.4	Experimental Setup	32
3.4.1	CST Microwave Studio (CST MWS)	32
3.4.2	Scattering Parameter (S11)	33
3.4.3	Far-field Radiation Pattern	34
3.5	Summary	36
<b>CHAPTER 4 RESULTS AND DISCUSSIONS</b>		<b>37</b>
4.1	Introduction	37
4.2	Results and Analysis	37
4.2.1	Calculations	37
4.2.2	Design procedure	38
4.2.2.1	Unit Cell Design	38
4.2.2.2	Horn Antenna Design	40
4.2.2.3	10x10 Reflectarray Design	41
4.2.2.4	10x10 Reflectarray Antenna with Horn Antenna Design	43
4.2.2.5	20x20 Reflectarray Antenna Design	43
4.2.2.6	20x20 Reflectarray Antenna with Horn Antenna Design	45
4.2.2.7	Fabricated Design of 20x20 Reflectarray	46
4.2.3	Results and Discussions	47
4.2.3.1	Unit Cell Antenna Design Results	47
4.2.3.2	Optimization of Horn Antenna	51
4.2.3.3	10x10 Reflectarray Antenna Design Results	52
4.2.3.4	20x20 Reflectarray Antenna Design Results	58
4.3	Summary	64
<b>CHAPTER 5 CONCLUSION AND RECOMMENDATIONS</b>		<b>66</b>
5.1	Conclusion	66
5.2	Future Works	67
<b>REFERENCES</b>		<b>69</b>
<b>APPENDICES</b>		<b>72</b>

## LIST OF TABLES

TABLE	TITLE	PAGE
Table 2.1	Summary Table of Literature Review	24



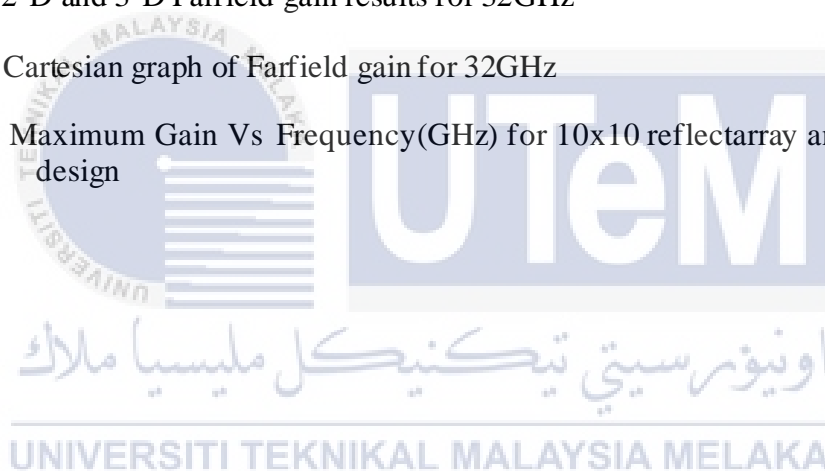
## LIST OF FIGURES

FIGURE	TITLE	PAGE
Figure 2.1	The setup for measuring the reflection phase and the prototype of a dual-band/dual-polarized array.	10
Figure 2.2	The radiation patterns for X-polarization were measured and simulated at two different frequencies. At frequency (a) $f_1$ of 28.7GHz and frequency (b) $f_2$ of 32.8GHz, both the measured and simulated radiation patterns were analyzed.	10
Figure 2.3	The arrangement of a massive multiple-input multiple-output (MIMO) array.	11
Figure 2.4	The normalized realized gain patterns of three array antennas were examined for switched beam scanning. The analysis included two different frequencies: (a) 28 GHz and (b) 38 GHz.	12
Figure 2.5	The shape and structure of an aperture-coupled E-shaped patch antenna	13
Figure 2.6	The three-dimensional radiation pattern of the optimal design was examined at two distinct frequencies: (a) 25 GHz and (b) 37 GHz.	13
Figure 2.7	Design of a Wideband Reflectarray Element for Dual Band Operation in 5G Communications	14
Figure 2.8	A prototype of the single-port dual-band antenna design under consideration	15
Figure 2.9	The radiation patterns of the prototype were both measured and simulated at two different frequency bands. (a) At frequencies of 4.83 and 4.9 GHz within the MW (Microwave) band. (b) At frequencies of 24.74 and 27.57 GHz within the MMW (Millimeter Wave) band.	16
Figure 2.10	The structure of the waveguide reflecting element and the mechanisms involved in scattering for both non-resonant and resonant modes	17
Figure 2.11	The dual-band reflectarray antenna exhibits radiation patterns on the two main planes at 28 and 60 GHz. In (a), the radiation pattern is observed at 28 GHz, while in (b), it is observed at 60 GHz. In both cases, the antenna beams are aligned with the antenna's boresight directions.	18
Figure 2.12	The design structure of a reflectarray and the arrangement of the feeding source.	19

Figure 2.13 The radiation patterns of the reflectarray antenna were both simulated and measured. The patterns were observed in the E-plane at three different frequencies: 42 GHz (a), 45 GHz (b), and 49 GHz (c). Additionally, the radiation patterns were also observed in the H-plane at the same three frequencies: 42 GHz (d), 45 GHz (e), and 49 GHz (f).	20
Figure 2.14 The conceptualization and development of an antenna design utilizing liquid crystal technology for reflection control	21
Figure 2.15 The reflectarray antenna exhibits a radiation pattern characterized by four beams.	21
Figure 2.16 The radiation characteristics of the suggested antenna array operating at frequencies of 28 GHz and 39.95 GHz.	22
Figure 2.17 The simulated radiation pattern of a 4-element linear array at 28 GHz and 38 GHz is analyzed in both the E-plane (with a fixed azimuthal angle of 90°) and the H-plane (with a fixed azimuthal angle of 0°)	23
Figure 3.1 Process flow of the project	32
Figure 3.2 Example image of CST MWS project design	33
Figure 3.3 S-Parameters in two port network	34
Figure 3.4 The far-field radiation patterns, along with their cross-sectional views in the E-plane and H-plane, are examined.	35
Figure 4.1 (a) Front view, (b) Back view, and (c) Bottom view of the unit cell design with dimensions for the length, width, and height of substrate, ground, and patch.	39
Figure 4.2 Parameter list of unit cell design	40
Figure 4.3 Boundary Conditions	40
Figure 4.4 Horn antenna design	41
Figure 4.5 Parameter list with dimensions of horn antenna	41
Figure 4.6 Lines and circles from curves	42
Figure 4.7 10x10 reflectarray design with dimensions	42
Figure 4.8 Parameter list of 10x10 reflectarray design	42

Figure 4.9 Design of the 10x10 reflectarray antenna with horn antenna	43
Figure 4.10 Lines and circles from curves	44
Figure 4.11 20x20 reflectarray design with dimensions	44
Figure 4.12 Parameter list of 20x20 reflectarray design	45
Figure 4.13 Design of the 20x20 reflectarray antenna with horn antenna	46
Figure 4.14 Front and back view of fabricated design	47
Figure 4.15 Design of the unit cell with port	47
Figure 4.16 Graph of S-Parameter for unit cell design	48
Figure 4.17 Graph of S-Parameter (Phase in Degree) for unit cell design after unwrapped	48
Figure 4.18 Graph of S-Parameter using parameter sweep for different length of patch unit cell	49
Figure 4.19 Graph of S-Parameter (Phase in Degree) using parameter sweep for different length of patch unit cell after unwrapped	50
Figure 4.20 Graph of Return Loss VS Length of Patch	51
Figure 4.21 Graph of Phase VS Length of Patch	51
Figure 4.22 Design of the horn antenna with port	52
Figure 4.23 Graph of S-Parameter for horn antenna design	52
Figure 4.24 Design of the 10x10 reflectarray and horn antenna with port	53
Figure 4.25 Graph of S-Parameter for 10x10 reflectarray antenna design	53
Figure 4.26 2-D and 3-D Farfield gain results for 24GHz	54
Figure 4.27 Cartesian graph of Farfield gain for 24GHz	54
Figure 4.28 2-D and 3-D Farfield gain results for 28GHz	55
Figure 4.29 Surface current for 28GHz	55
Figure 4.30 Cartesian graph of Farfield gain for 28GHz	56
Figure 4.31 2-D and 3-D Farfield gain results for 32GHz	57
Figure 4.32 Cartesian graph of Farfield gain for 32GHz	57

Figure 4.33 Maximum Gain Vs Frequency(GHz) for 10x10 reflectarray antenna design	58
Figure 4.34 Design of the 20x20 reflectarray antenna with port	59
Figure 4.35 Graph of S-Parameter for 20x20 reflectarray antenna design	59
Figure 4.36 2-D and 3-D Farfield gain results for 24GHz	60
Figure 4.37 Cartesian graph of Farfield gain for 24GHz	60
Figure 4.38 2-D and 3-D Farfield gain results for 28GHz	61
Figure 4.39 Surface current for 28GHz	61
Figure 4.40 Cartesian graph of Farfield gain for 28GHz	62
Figure 4.41 2-D and 3-D Farfield gain results for 32GHz	63
Figure 4.42 Cartesian graph of Farfield gain for 32GHz	63
Figure 4.43 Maximum Gain Vs Frequency(GHz) for 10x10 reflectarray antenna design	64



## LIST OF APPENDICES

APPENDIX	TITLE	PAGE
Appendix A	Gantt Chart For Final Year Project 1	72
Appendix B	Gantt Chart For Final Year Project 2	73



# CHAPTER 1

## INTRODUCTION

### 1.1 Background

The development of 5G communication systems has been prompted by the evolution of wireless communication systems and the expanding demand for quick data transmission. These systems require advanced antenna technologies to enable reliable and high-capacity wireless communication. Reflectarray antennas have emerged as a promising solution due to their ability to provide beamforming and beam-steering capabilities, allowing for efficient signal transmission and reception[1].

This project focuses on the design of a millimeter wave reflectarray antenna operating at 28 GHz frequency, specifically tailored for 5G communication systems. The antenna's resonance property allows for efficient operation in the 28 GHz frequency band, providing flexibility in communication applications and ensuring compatibility with the latest 5G standards. Millimeter waves (mmwaves), encompassing frequencies from 30 to 300 gigahertz, have emerged as a transformative force in wireless communication. Particularly notable in the context of 5G networks, these waves enable unprecedented data transmission speeds, low latency, and enhanced network capacity. The deployment of millimeter-wave frequencies is pivotal in addressing the escalating demands for high-speed, data-intensive communication systems. Beyond telecommunications, millimeter-wave technology finds applications in imaging, sensing, and radar systems, thanks to its unique characteristics such as high resolution and material penetration capabilities. Researchers and engineers continually explore innovative solutions, including the optimization of antennas

like reflectarray antennas, to efficiently utilize and advance millimeter-wave technology. This evolution marks a crucial era in wireless communication and broader technological domains, unlocking new frontiers and possibilities.

To accomplish the antenna design, the Computer Simulation Technology (CST) software will be utilized. CST provides a powerful platform for electromagnetic simulation and analysis, enabling accurate modeling and evaluation of antenna performance. The software's comprehensive features, such as its ability to handle complex geometries, simulate different materials, and analyze radiation patterns, make it an ideal tool for designing reflectarray antennas.

The successful implementation of this project will result in the design of a millimeter-wave reflectarray antenna for 5G communication systems. The antenna's unique properties, such as its single-band operation and beam-steering capabilities, will contribute to the advancement of wireless communication technologies, enabling efficient and reliable communication in the 5G era. The CST software will play a vital role in the design and evaluation process, facilitating accurate simulation and optimization of the antenna's performance parameters.

## **1.2 Global and Societal Issues**

It aims to identify the key challenges and considerations that arise from the antenna design and its impact on a global scale, as well as its societal implications. The report focuses on two main areas: global issues, which encompass broader environmental concerns and the digital divide, and societal issues, which include health and safety considerations, as well as affordability and accessibility factors.

The deployment of 5G communication systems, including antennas, has significant global implications. One of the main concerns is the environmental impact, as the increased

energy consumption and resource demands associated with 5G technology can contribute to environmental degradation. The project should prioritize sustainability principles in the antenna design process to minimize its environmental footprint and promote efficient resource utilization. Additionally, the digital divide poses a challenge, with unequal access to 5G communication systems across different regions and communities. The project should aim to bridge this divide by considering the societal implications of the antenna design, ensuring equitable access to 5G technology and fostering inclusivity.

A critical societal issue to address in the project is the potential health and safety risks associated with 5G antennas. Concerns have been raised regarding the effects of prolonged exposure to electromagnetic radiation. It is essential for the project to adhere to safety regulations and guidelines, designing the reflectarray antenna to minimize any potential health risks for users and the surrounding environment. Moreover, affordability and accessibility are significant considerations. The high costs of 5G technology can create barriers to access, particularly in economically disadvantaged areas. The project should take affordability and accessibility factors into account to develop a cost-effective antenna solution that promotes wider adoption of 5G communication systems, ensuring inclusivity and accessibility for all.

### 1.3 Challenges

Several key challenges need to be addressed in this project:

- a) **Millimeter Wave Design:** Designing a millimeter wave reflectarray antenna capable of operating at 28 GHz frequency poses a technical challenge. Achieving the required phase shifts across the antenna aperture for optimal operation is crucial, requiring careful design optimization and accurate modelling.

- b) **Radiation Pattern Optimization:** Ensuring a high-gain and directive radiation pattern is essential for efficient signal transmission and reception in 5G communication systems. Designing the reflectarray elements to achieve the desired radiation properties, including beam-steering capabilities, necessitates precise modelling and optimization techniques.
- c) **Bandwidth and Performance Requirements:** The reflectarray antenna needs to meet the specific bandwidth and performance requirements for 5G communication systems. This includes achieving sufficient bandwidth, low return loss, and minimizing cross-polarization levels to enhance the antenna's performance and compatibility with 5G standards.

Addressing these challenges is critical for the successful design of a millimeter wave reflectarray antenna using CST software. The project seeks to overcome these obstacles and deliver a well-optimized antenna design that meets the demands of 5G communication systems, providing efficient and reliable wireless connectivity for various applications in the 5G era[2].

#### 1.4 Problem Statement

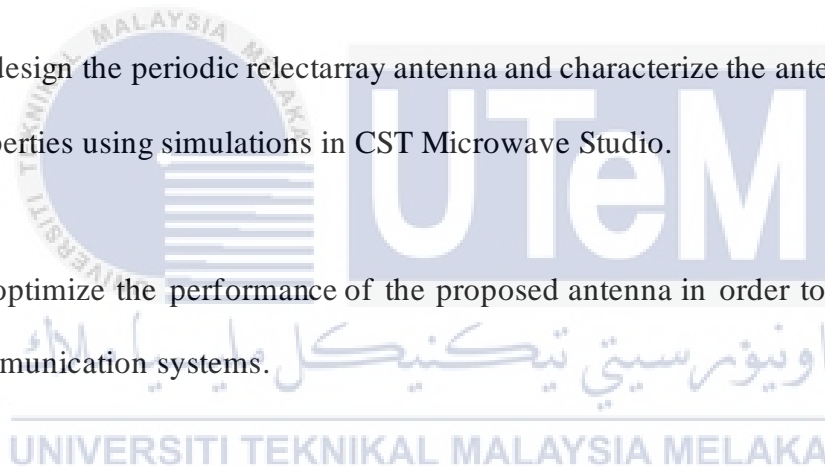
The rapid growth and increasing demand for high-speed data transfer in wireless communication systems have necessitated the development of advanced antenna technologies for 5G communication systems. The design and implementation of a millimeter-wave reflectarray antenna operating at 28 GHz frequency pose a significant challenge. The problem at hand lies in achieving efficient beamforming and beam-steering capabilities, along with optimal radiation properties, to enable reliable and high-capacity

wireless communication in 5G networks. In this work, an optimum performance reflectarray antenna has been proposed with a resonance operating at 28 GHz for 5G communication systems.

## 1.5 Project Objective

The project aims to achieve the following objectives:

- a) To design a millimeter wave reflectarray unit cell and optimize the performance based on scattering parameter results.
- b) To design the periodic reflectarray antenna and characterize the antenna's radiation properties using simulations in CST Microwave Studio.
- c) To optimize the performance of the proposed antenna in order to use it for 5G communication systems.



## 1.6 Scope and Limitations of Project

**The following is the project's scope:**

- The project aimed to design a millimeter-wave reflectarray antenna operating at a frequency of 28 GHz.
- The antenna was intended for use in 5G communication systems to provide high-speed data transmission and improved network coverage.
- For the development, simulation, and evaluation of the reflectarray antenna for the project, CST software was used.

- The development focused on optimizing the antenna's radiation characteristics, gain, directivity, and bandwidth at the specified operating frequency of 28 GHz.
- The project considered various design parameters such as reflectarray element shape, size, spacing, and phase distribution.
- Performance evaluation of the designed antenna was carried out using simulation tools and compared against desired specifications.

**The limitation of this project are as follows:**

- The project was limited to the design and simulation of the reflectarray antenna using CST software. It did not include the complete fabrication and prototyping process.
- The project assumed ideal environmental conditions and isotropic radiation patterns. Real-world conditions and practical considerations were not fully addressed.
- The reflectarray design was based on the specific operating frequency of 28 GHz, limiting its application to that frequency only.
- The project did not consider the effects of neighboring antennas, mutual coupling, or interference from other sources, which could affect the overall performance.
- The accuracy of the simulation results was dependent on the accuracy of the input parameters, material properties, and simulation models used in the CST software.
- The project did not explore all possible design variations or optimizations due to time and resource constraints.
- If conducted, the experimental validation of the antenna design may have had limitations such as measurement inaccuracies, fabrication tolerances, and environmental effects[3].

## 1.7 Summary

This project focused on designing a millimeter-wave reflectarray antenna for 5G communication at a frequency of 28 GHz. The aim was to address challenges related to reflectarray design, radiation pattern optimization, and meeting performance requirements. By utilizing Computer Simulation Technology (CST) software, the project aimed to achieve accurate modeling and evaluation of the antenna's performance. Objectives included designing and optimizing unit cells, creating the periodic reflectarray antenna, and simulating its radiation properties. The project's scope covered antenna design, CST software utilization for simulation and analysis, and optimizing radiation characteristics and performance. Limitations included the exclusion of fabrication and prototyping, ideal environmental assumptions, and neglecting neighboring antenna effects and interference. Successful implementation contributed to wireless communication advancements, providing an optimized millimeter-wave reflectarray antenna for 5G systems, with CST software playing a crucial role in accurate simulation and optimization.

## CHAPTER 2

### LITERATURE REVIEW

#### 2.1 Introduction

In The demand for high-speed, low-latency, and reliable communication has increased significantly with the advent of fifth generation (5G) communication systems. Reflectarray antennas have emerged as a promising solution for 5G communication due to their unique features such as high gain, low profile, and wideband operation. Reflectarray antennas designed for millimeter-wave frequencies have attracted considerable attention, with a particular focus on their ability to operate at multiple frequencies and polarization states simultaneously. In this literature review, we will examine the recent developments in the design and analysis of 28 GHz reflectarray antennas for 5G communication, with a focus on the key challenges and opportunities associated with this emerging technology [4].

#### 2.2 5G Communications Systems

Over the years, the field of communication has witnessed remarkable progress, and one of the most significant advancements is the introduction of the 5G communication system. 5G, also known as the fifth generation of wireless technology, is transforming the way we connect and communicate, offering lightning-fast speeds, ultra-low latency, and extensive connectivity. This revolutionary technology is paving the path for a new era of innovation and digital transformation[5].

The evolution of mobile communication began with the emergence of the first generation (1G) in the 1980s, which facilitated basic voice calls but lacked data capabilities. Subsequently, the second generation (2G) brought forth digital networks, enabling text

messaging and introducing the concept of roaming. A major milestone was achieved with the arrival of the third generation (3G), which provided mobile internet access, faster data speeds, and the ability to make video calls. However, these early generations primarily focused on voice and had limited data services[5].

The introduction of the fourth generation (4G) marked a significant leap for mobile networks, delivering substantial improvements in speed, capacity, and data capabilities. With 4G, users gained faster internet browsing, video streaming, and access to mobile applications. Nevertheless, as the demand for more advanced services grew, the limitations of 4G became evident. This led to the development of the fifth generation (5G), which surpasses its predecessors on multiple fronts. 5G offers unmatched speeds, ultra-low latency, and increased capacity, positioning it as the foundation for cutting-edge technologies like autonomous vehicles, IoT devices, smart cities, and augmented reality. Moreover, 5G utilizes advanced technologies such as network slicing and beamforming to ensure efficient resource utilization and improved connectivity, even in densely populated areas [20].

## **2.3 Reflectarray for 5G communications**

### **2.3.1 Dual-Band Dual-Linear Polarization Reflectarray for mmWaves/5G Applications**

The article "Dual-Band Dual-Linear Polarization Reflectarray for mmWaves/5G Applications" proposed by Costanzo et al. (2019) presents a dual-band dual-linear polarization reflectarray antenna with square patches printed on a thin substrate with a ground plane. The antenna operates at 28 GHz and 38 GHz, providing a gain of 19.2 dBi and 20.6 dBi, respectively. The dual-linear polarization feature of the antenna helps to improve the system capacity and reduce the effect of polarization mismatch. The antenna's design involves adjusting the patch size and spacing to achieve dual-band operation and using the

polarization rotation technique to achieve dual-linear polarization. The simulation results showed that the proposed antenna has a high gain, low sidelobe level, and good radiation pattern. Although this antenna is a viable option for mmWaves/5G applications, more study is necessary to improve the layout and efficiency of these antennas for various scenarios and applications[6].

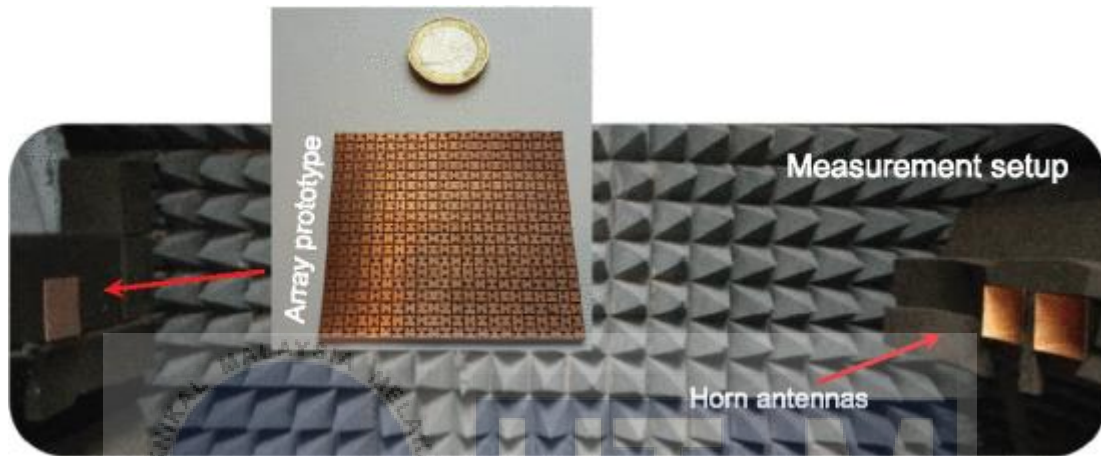


Figure 2.1 The setup for measuring the reflection phase and the prototype of a dual-band/dual-polarized array.

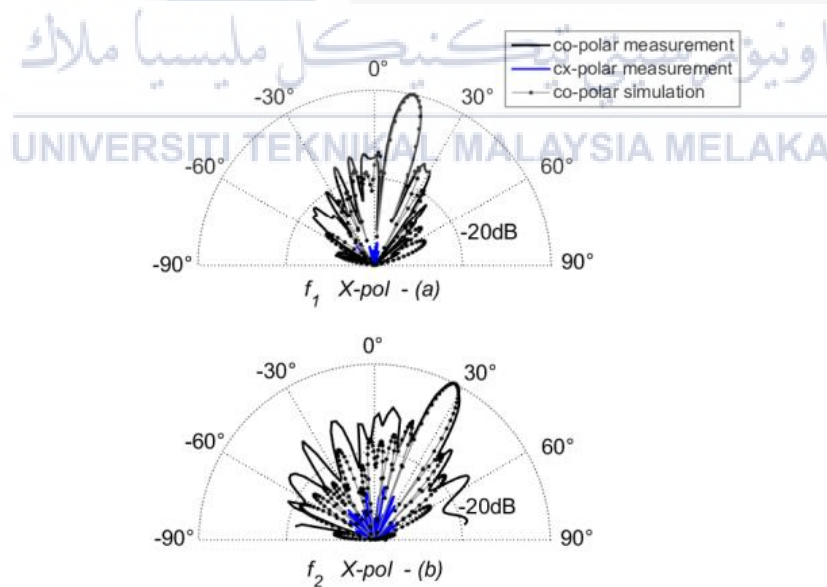


Figure 2.2 The radiation patterns for X-polarization were measured and simulated at two different frequencies. At frequency (a)  $f_1$  of 28.7GHz and frequency (b)  $f_2$  of 32.8GHz, both the measured and simulated radiation patterns were analyzed.

### 2.3.2 Design of compact millimeter wave massive MIMO dual-band (28/38 GHz) antenna array for future 5G communication systems

Ali et al. (2016) proposed a compact dual-band massive MIMO antenna array for future 5G communication systems. The design consists of a 4x4 antenna array that operates at 28 GHz and 38 GHz, with a compact size of 10x10 mm<sup>2</sup>. The authors used a corporate feeding technique and substrate-integrated waveguide (SIW) structure to improve the antenna's performance, resulting in a reduced size and mutual coupling. The simulation results showed that the proposed antenna array has a good impedance bandwidth, low mutual coupling, and high gain, outperforming the traditional patch antenna array. This antenna array is a promising solution for future 5G communication systems, but further research is needed to optimize its design and performance for different applications and scenarios[7].

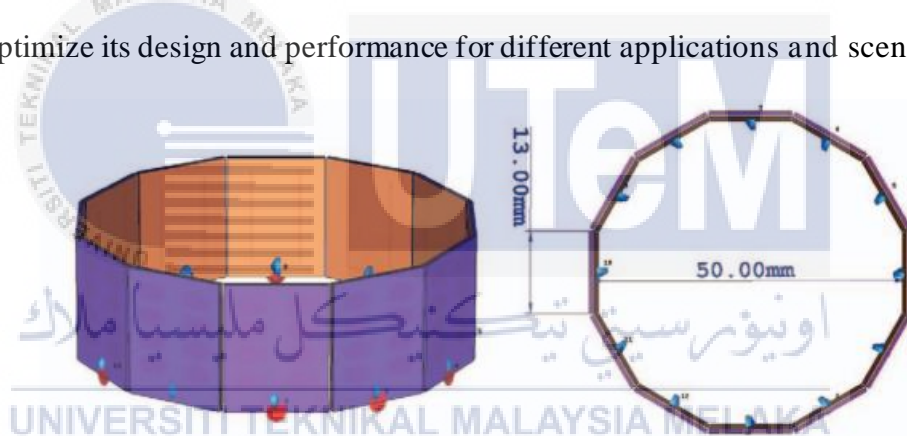


Figure 2.3 The arrangement of a massive multiple-input multiple-output (MIMO) array.

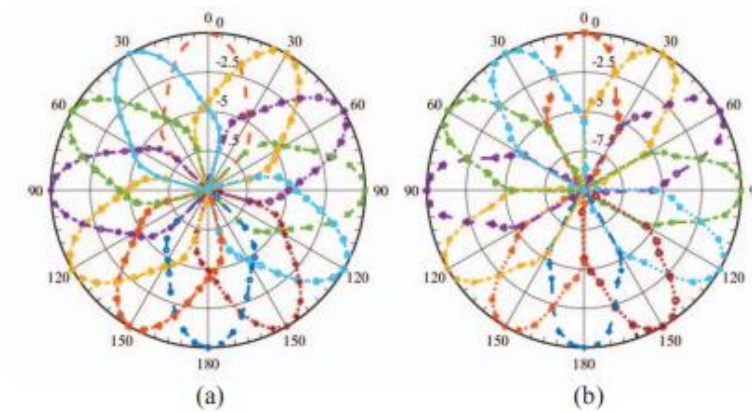


Figure 2.4 The normalized realized gain patterns of three array antennas were examined for switched beam scanning. The analysis included two different frequencies: (a) 28 GHz and (b) 38 GHz.

### 2.3.3 Evolutionary design of a dual band E-shaped patch antenna for 5G mobile communications

The project "Evolutionary design of a dual band E-shaped patch antenna for 5G mobile communications" proposed by Goudos et al. (2020) presents an evolutionary design method for applications in need of a 5G mobile communication dual-band E-shaped patch antenna. The antenna operates at 3.5 GHz and 28 GHz with a good impedance bandwidth, gain, and radiation pattern. The authors used the Genetic Algorithm (GA) to optimize the design of the antenna. According to the simulation results, the proposed antenna performs better when it comes to bandwidth of impedance and gain than the conventional rectangular patch antenna. This study provides a promising solution for 5G mobile communication applications by using the E-shaped patch antenna, which is known for its low profile, simple design, and easy integration with a mobile device. To improve the design and functionality of these antennas for a variety of scenarios and applications, more study is necessary [8].

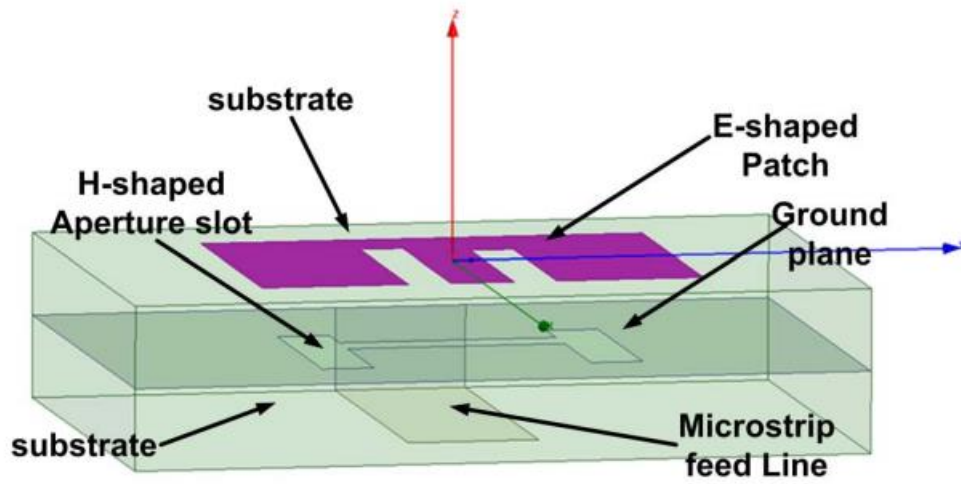


Figure 2.5 The shape and structure of an aperture-coupled E-shaped patch antenna

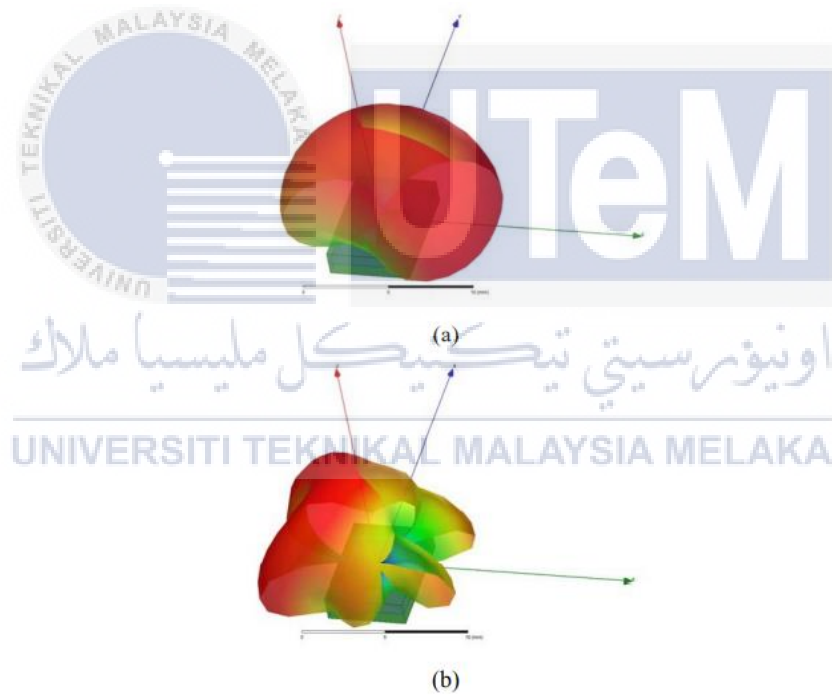


Figure 2.6 The three-dimensional radiation pattern of the optimal design was examined at two distinct frequencies: (a) 25 GHz and (b) 37 GHz.

### 2.3.4 Design of a Wideband Reflectarray Element for Dual Band Operation in 5G Communications

The project "Design of a Wideband Reflectarray Element for Dual Band Operation in 5G Communications" proposed by Bashir et al. (2021) presents the design of a wideband reflectarray element for dual-band operation in 5G communications. The proposed element is designed to operate at two frequency bands: 3.3-3.6 GHz and 26.5-29.5 GHz. The authors used a circular patch with a cross-shaped slot as the radiating element and a four-arm spiral feed for improved performance. The proposed reflectarray element showed a wideband impedance bandwidth of 12.4% at the lower band and 15.4% at the higher band, as well as a high gain and low cross-polarization level. The proposed element is a promising solution for dual-band operation in 5G communications, but further research is needed to optimize its design and performance for different applications and scenarios[9].

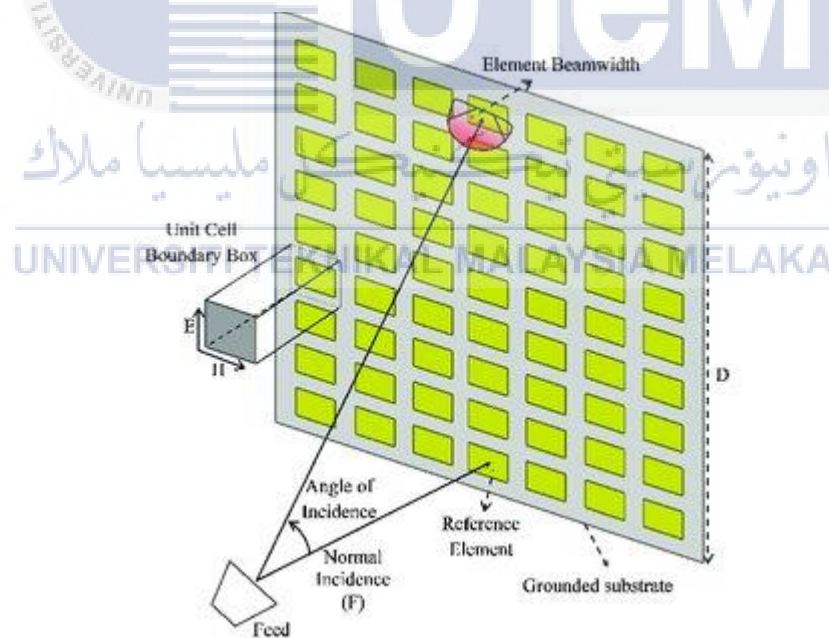


Figure 2.7 Design of a Wideband Reflectarray Element for Dual Band Operation in 5G Communications

### 2.3.5 A singly fed dual-band microstrip antenna for microwave and millimeter-wave applications in 5G wireless communication

The project "A singly-fed dual-band microstrip antenna for microwave and millimeter-wave applications in 5G wireless communication" proposed by Guo et al. (2021) presents the design and analysis of a singly fed dual-band microstrip antenna for microwave and millimeter-wave applications in 5G wireless communication systems. The proposed antenna consists of a rectangular patch with a T-shaped feed line on a substrate with a ground plane. The antenna operates at two frequency bands, 3.3-3.7 GHz and 27.2-30 GHz, with a compact size and high radiation efficiency. The simulation and measurement results demonstrated the proposed antenna's excellent performance, with a maximum gain of 7.2 dBi and 10.7 dBi at the lower and higher bands, respectively. The proposed antenna's compact size, low profile, and low cost make it a promising solution for 5G wireless communication systems, particularly for mobile and portable devices. However, further research is needed to optimize the proposed antenna's performance for different applications and scenarios[10].

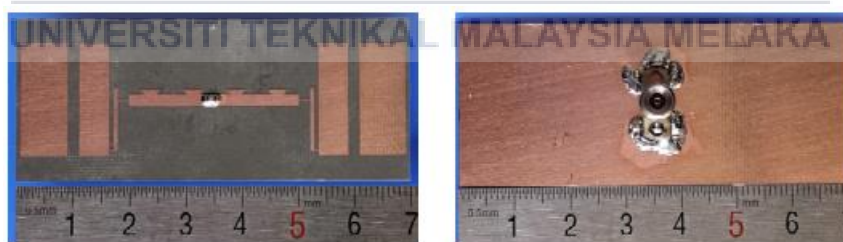


Figure 2.8 A prototype of the single-port dual-band antenna design under consideration

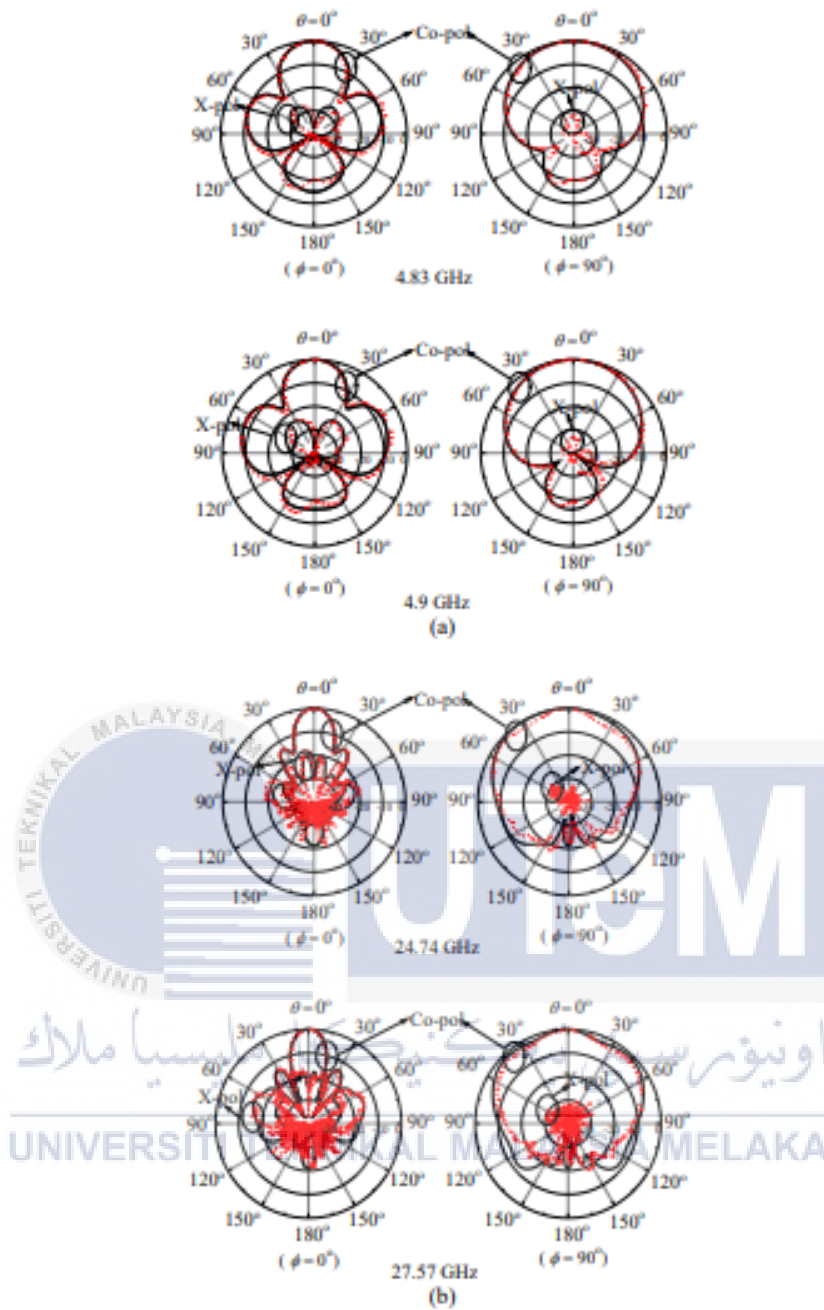


Figure 2.9 The radiation patterns of the prototype were both measured and simulated at two different frequency bands. (a) At frequencies of 4.83 and 4.9 GHz within the MW (Microwave) band. (b) At frequencies of 24.74 and 27.57 GHz within the MMW (Millimeter Wave) band.

### 2.3.6 Dual-Band Reflectarray Antennas Using Integrated Resonant and Non-Resonant Natures of Metallic Waveguide Elements at Millimeter Wave Frequencies

The project "Dual-Band Reflectarray Antennas Using Integrated Resonant and Non-Resonant Natures of Metallic Waveguide Elements at Millimeter Wave Frequencies" proposed by Chou et al. (2023) presents a novel approach to designing dual-band reflectarray antennas for millimeter-wave frequencies. The authors used a combination of resonant and non-resonant metallic waveguide elements to achieve two operating frequencies, namely 28 GHz and 38 GHz. The proposed antennas demonstrated excellent performance in terms of gain, efficiency, and return loss, with a maximum gain of 20 dBi and a bandwidth of 3.1 GHz at the lower band and 2.8 GHz at the higher band. The proposed approach is a promising solution for designing dual-band reflectarray antennas for 5G and other millimeter-wave communication systems, particularly for applications requiring high gain, low profile, and wideband operation. To optimise the structure and efficiency of these types of antennas for various scenarios and applications, additional study is necessary [11].

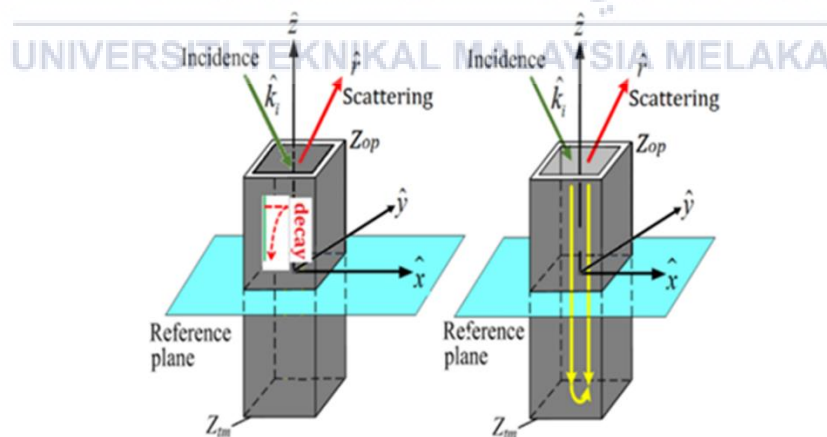
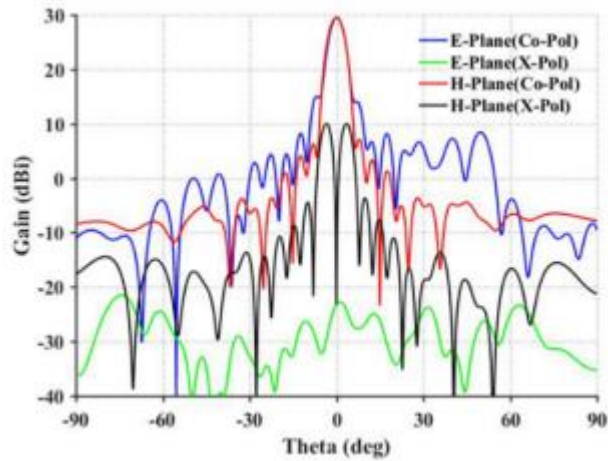
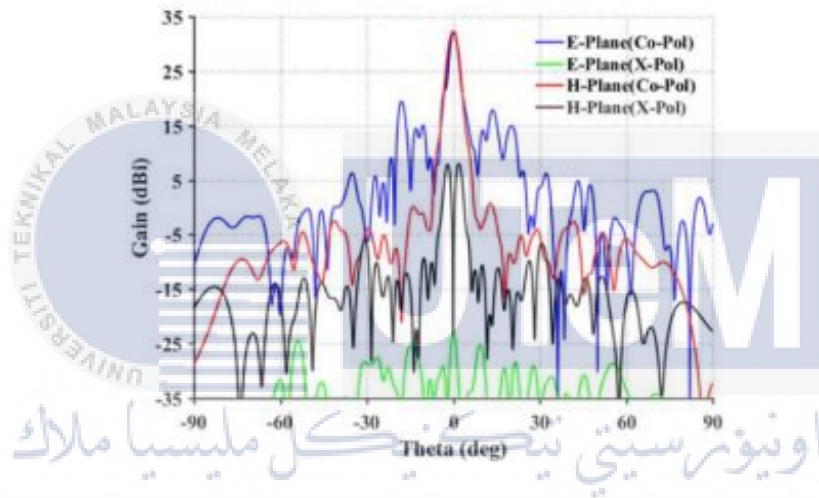


Figure 2.10 The structure of the waveguide reflecting element and the mechanisms involved in scattering for both non-resonant and resonant modes



(a)



(b)

Figure 2.11 The dual-band reflectarray antenna exhibits radiation patterns on the two main planes at 28 and 60 GHz. In (a), the radiation pattern is observed at 28 GHz, while in (b), it is observed at 60 GHz. In both cases, the antenna beams are aligned with the antenna's boresight directions.

### 2.3.7 Wideband Millimeter-Wave Microstrip Reflectarray Using Dual-Resonance Unit Cells

In this literature review, the research conducted by the authors Xiaoyue et al. (2019) focuses on a wideband millimeter-wave reflectarray antenna. The review investigates the proposed design scheme, which begins with the introduction of a new dual-resonance unit cell utilizing the microstrip technique. This unit cell offers an approximately linear phase response range of  $0^{\circ}$ - $360^{\circ}$  and exhibits nearly parallel phase response curves within a broad band, resulting in an expanded operating bandwidth for the reflectarray antenna. Subsequently, the authors design, fabricate, and measure a reflectarray antenna consisting of 1296 of these proposed unit cells. The measured results demonstrate a boresight gain of 31.9 dBi and a 1-dB bandwidth exceeding 29.3% at Q-band. Furthermore, the simulation and measurement results align remarkably well with the proposed design scheme, confirming the efficacy of the wideband millimeter-wave reflectarray antenna. Overall, this literature review highlights the significance of the authors' contributions in developing a wideband millimeter-wave reflectarray antenna with enhanced performance and validates their findings through thorough experimental measurements [12].

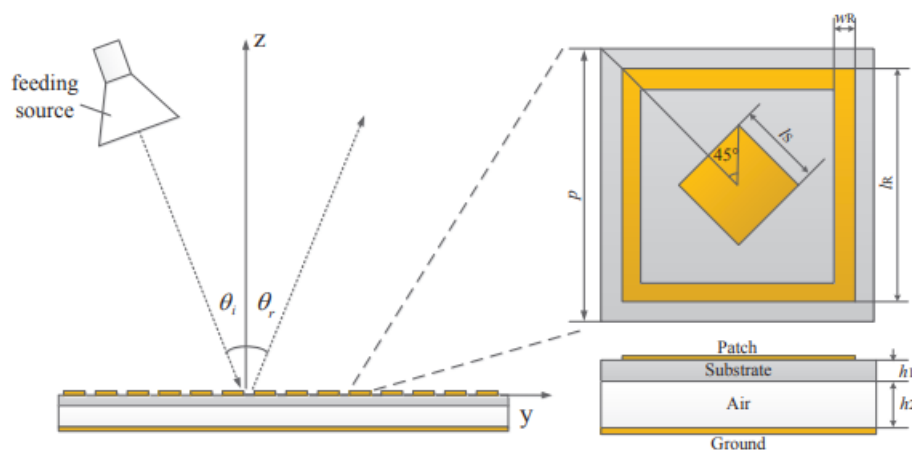


Figure 2.12 The design structure of a reflectarray and the arrangement of the feeding source.

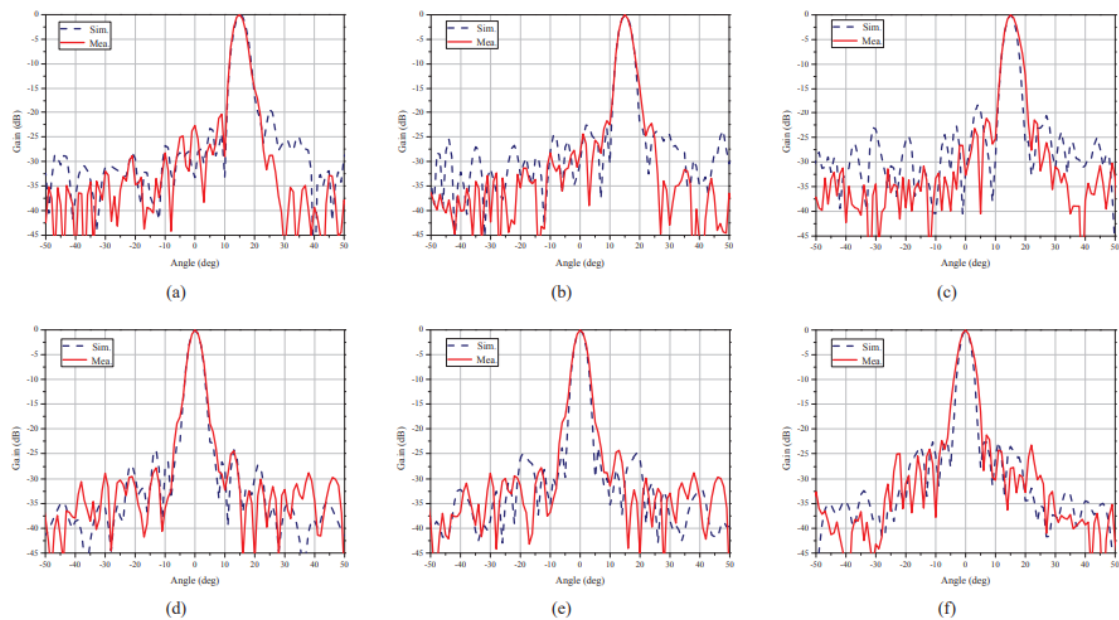


Figure 2.13 The radiation patterns of the reflectarray antenna were both simulated and measured. The patterns were observed in the E-plane at three different frequencies: 42 GHz (a), 45 GHz (b), and 49 GHz (c). Additionally, the radiation patterns were also observed in the H-plane at the same three frequencies: 42 GHz (d), 45 GHz (e), and 49 GHz (f).

### 2.3.8 Polarization Diversity and Adaptive Beamsteering for 5G Reflectarrays: A Review

The literature review titled "Polarization Diversity and Adaptive Beamsteering for 5G Reflectarrays: A Review" by Dahri et al. (2018) provides an overview of polarization diversity and adaptive beamsteering techniques for 5G reflectarray antennas. The authors delve into the challenges and opportunities associated with achieving efficient beamsteering capabilities and polarization diversity in reflectarrays, which are crucial for 5G communication systems. The review explores various approaches and methodologies proposed in the literature, including the use of polarization rotators, multi-layer structures, and reconfigurable reflectarrays. The authors discuss the advantages and limitations of each technique, highlighting their potential to enhance the performance of 5G reflectarray antennas in terms of beam agility, polarization adaptation, and coverage. Through a comprehensive analysis of existing research, this review offers valuable insights into the

state-of-the-art techniques for polarization diversity and adaptive beamsteering in reflectarray antennas, enabling researchers and engineers to make informed decisions in the design and optimization of 5G communication systems[13].

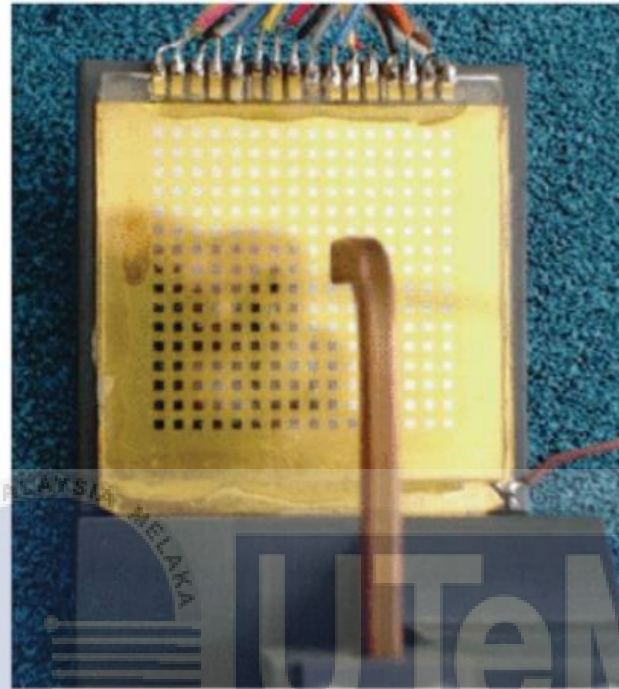


Figure 2.14 The conceptualization and development of an antenna design utilizing liquid crystal technology for reflection control

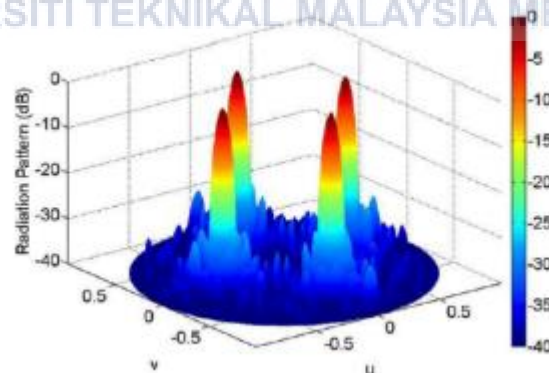


Figure 2.15 The reflectarray antenna exhibits a radiation pattern characterized by four beams.

### 2.3.9 Dual-band microstrip patch antenna array for 5G mobile communication

The research paper titled "Dual-band microstrip patch antenna array for 5G mobile communications" by Rafique et al. (2017) presents a study on the design and development of a dual-band microstrip patch antenna array specifically tailored for 5G mobile communications. The authors focus on addressing the growing demand for higher data rates and increased bandwidth in 5G networks. They propose a novel approach of using a dual-band microstrip patch antenna array, which operates at two different frequency bands, to achieve enhanced performance and coverage. The paper discusses the design considerations, including the selection of substrate materials, feeding techniques, and array configuration. The authors also provide simulation results and performance evaluations of the proposed antenna array, demonstrating its capability to cover the desired frequency bands for 5G mobile communications. This research contributes to the advancement of antenna technologies for 5G networks, offering a potential solution for achieving dual-band operation and improved performance in mobile communication systems[14].

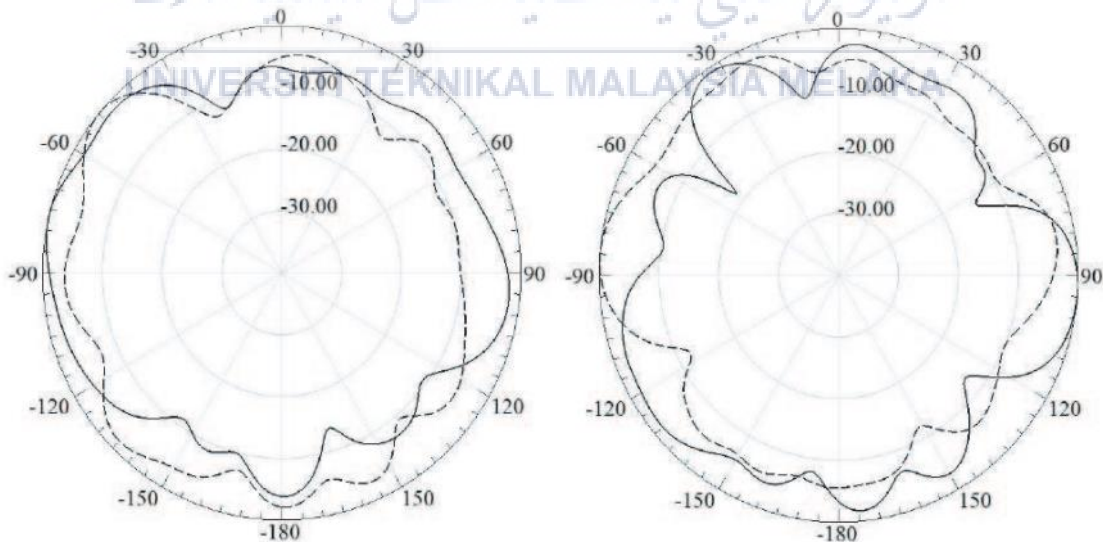


Figure 2.16 The radiation characteristics of the suggested antenna array operating at frequencies of 28 GHz and 39.95 GHz.

### 2.3.10 Dual-Band (28,38) GHz Coupled Quarter-Mode Substrate-Integrated Waveguide Antenna Array for Next-Generation Wireless Systems

The literature review titled "Dual-Band (28,38) GHz Coupled Quarter-Mode Substrate-Integrated Waveguide Antenna Array for Next-Generation Wireless Systems" by Deckmyn et al. (2019) focuses on the design and implementation of a dual-band (28,38) GHz coupled quarter-mode substrate-integrated waveguide (QMSIW) antenna array for next-generation wireless systems. The authors address the increasing demand for higher data rates and improved capacity in wireless communication networks. They propose a novel approach of using coupled QMSIW elements to achieve dual-band operation, specifically targeting the 28 GHz and 38 GHz frequency bands. The paper discusses the design considerations, including the choice of substrate, the geometry of the QMSIW elements, and the coupling mechanism. Simulation results and performance evaluations are presented to demonstrate the effectiveness of the proposed antenna array in terms of radiation patterns, gain, and bandwidth. This research contributes to the development of antenna technologies for next-generation wireless systems, offering a potential solution for achieving dual-band operation and improved performance in high-frequency wireless communication applications[15].

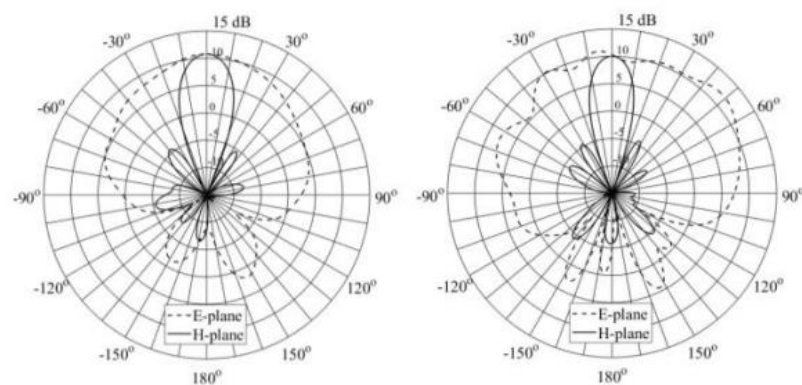


Figure 2.17 The simulated radiation pattern of a 4-element linear array at 28 GHz and 38 GHz is analyzed in both the E-plane (with a fixed azimuthal angle of  $90^\circ$ ) and the H-plane (with a fixed azimuthal angle of  $0^\circ$ )

## 2.4 Table of Literature Review

Table 2.1 Summary Table of Literature Review

NO.	TITLE	AUTHOURS	YEAR	ADVANTAGE	DISADVANTAGE
1	Dual-Band Dual-Linear Polarization Reflectarray for mmWaves/5G Applications	S. Costanzo, F. Venneri, A. Borgia, G. Di Massa	2019	Small Cell Size and Thin Structure	Limited Bandwidth
2	Design of compact millimeter wave massive MIMO dual-band (28/38 GHz) antenna array	Mohamed Mamdouh M. Ali, Abdel-Razik Sebek	2016	High Gain	Limited Azimuthal Coverage

	for future 5G communication systems				
3	Evolutionary design of a dual band E-shaped patch antenna for 5G mobile communications	S. K. Goudos, A. Tsiflikiotis, D. Babas, K. Siakavara, C. Kalialakis, G. K. Karagiannidis	2020	Optimization Algorithm	Limited Bandwidth
4	Design of a Wideband Reflectarray Element for Dual Band Operation in 5G Communications	Shanza Bashir, M. Hashim Dahri, Syed Nazim Shah, Jamal Nasir	2021	Progressive Phase Distribution	Limited Frequency Coverage

5	<p>A singly fed dual-band microstrip antenna for microwave and millimeter-wave applications in 5G wireless communication</p>	<p>Yu Qing Guo, Yong Mei Pan, Shao Yong Zheng, Kai Lu</p>	2021	<p>Dual-Band Operation</p>	Limited Bandwidth
6	<p>Dual-Band Reflectarray Antennas Using Integrated Resonant and Non-Resonant Natures of Metallic Waveguide Elements</p>	<p>H.-T. Chou, N.-N. Wang, M. Fang, L.-Q. Wang, P. Akkaraekthalin, D. Torrungrueng</p>	2023	<p>Millimeter Wave Frequency Range</p>	Limited Bandwidth

	at Millimeter Wave Frequencies				
7	Wideband Millimeter-Wave Microstrip Reflectarray Using Dual-Resonance Unit Cells	Xiaoyue Xia, Qi Wu, Haiming Wang, Chen Yu, Wei Hong	2019	Enhanced Bandwidth	Complexity of Unit Cell Design
8	Polarization Diversity and Adaptive Beamsteering for 5G Reflectarrays: A Review	Muhammad Hashim Dahri, Mohd Haizal Jamaluddin, Mohsen Khalily, Muhammad Inam Abbasi, Raghuraman Selvaraju, and	2018	Increased Network Flexibility	Cost Considerations

		Muhammad Ramlee Kamarudin			
9	Dual-band microstrip patch antenna array for 5G mobile communications	Umair Rafique, Hisham Khalil, Saif-Ur- Rehman	2017	Compact Size	Narrow Bandwidth
10	Dual-Band (28,38) GHz Coupled Quarter-Mode Substrate-Integrated Waveguide Antenna Array for Next- Generation Wireless Systems	Thomas Deckmyn, Maarten Cauwe, Dries Vande Ginste, Hendrik Rogier, Sam Agneessens	2019	Coupled Quarter-Mode Substrate-Integrated Waveguide (QM-SIW) Technology	Limited Frequency Range

## 2.5 Summary

The demand for high-speed, low-latency, and reliable communication in 5G systems has led to the emergence of millimeter wave reflectarray antennas as a promising solution. This literature review examines recent developments in the design and analysis of millimeter wave reflectarray antennas for 5G communication. Various research studies are reviewed, including the design of dual-band reflectarray antennas, compact antenna arrays, evolutionary design methods, wideband reflectarray elements, microstrip antennas, and dual-band reflectarray antennas using metallic waveguide elements. The review also covers polarization diversity, adaptive beamsteering techniques, and dual-band microstrip patch antenna arrays for 5G communication. The studies highlight the advantages and challenges associated with these antenna designs, providing insights into their potential for enhancing the performance of 5G communication systems.



## CHAPTER 3

### METHODOLOGY

#### 3.1 Introduction

There are numerous crucial elements in the design process for a millimeter wave reflectarray antenna operating at 28GHz for 5G communication systems. The Computer Simulation Technology (CST) software is used for designing, simulating, and analyzing the antenna. The first step is to optimize the unit cells, which are the basic building blocks of the reflectarray antenna. Through iterative design and optimization using CST, the unit cells are fine-tuned to achieve resonance at the desired frequency.

Once the unit cells are optimized, the next step is to design the periodic reflectarray structure. The arrangement of the unit cells in a periodic pattern allows for beamforming and beam-steering capabilities, enabling efficient signal transmission and reception. The CST software is utilized to simulate the electromagnetic behavior of the reflectarray and analyze its scattering parameters, specifically S11. This parameter provides insights into the antenna's impedance matching and helps assess its performance in terms of power reflection.

Additionally, the far-field radiation pattern of the reflectarray antenna is characterized through simulation. The CST software enables the analysis and optimization of the radiation pattern, which describes the antenna's directional radiation properties. By adjusting the design parameters in CST, such as the reflectarray's shape and size, the radiation pattern can be optimized to achieve the desired beam shape, gain, and beamwidth[7].

In summary, the design methodology for the millimeter wave reflectarray antenna for 5G communication systems involves optimizing the unit cells, designing the periodic

reflectarray structure, and characterizing the far-field radiation pattern. The CST software plays a crucial role in all these steps, providing accurate modeling, simulation, and analysis capabilities for efficient design optimization and performance assessment of the reflectarray antenna.

### **3.2 Sustainability Development**

This sustainability development report aims to integrate sustainability principles into the design of a millimeter wave reflectarray antenna for 5G communication systems. The key considerations include material selection, energy efficiency, life cycle assessment, e-waste management, radiation efficiency, compliance with regulations, and social impact.

Material selection focuses on prioritizing environmentally friendly and sustainable materials, such as recyclable low-impact polymers or biodegradable composites, to reduce the antenna's environmental footprint. Energy efficiency involves optimizing power consumption through energy-saving components and design techniques, contributing to a more efficient 5G communication system.

Conducting a life cycle assessment evaluates the environmental impact from raw material extraction to end-of-life disposal. Improvements can be identified, such as reducing energy consumption during manufacturing and implementing effective recycling practices. E-waste management emphasizes designing the antenna for easy disassembly and recyclability, with proper guidelines and protocols for responsible disposal.

Radiation efficiency optimization aims to reduce power requirements by refining the antenna's design and dimensions, while compliance with environmental regulations ensures sustainable practices throughout its life cycle. The social impact assessment focuses on bridging the digital divide and providing equitable access to 5G communication systems, considering factors like affordability and accessibility.

By integrating these sustainability considerations, the project can minimize environmental impact, optimize energy efficiency, and promote responsible practices throughout the antenna's life cycle.

### 3.3 Flowchart of this project

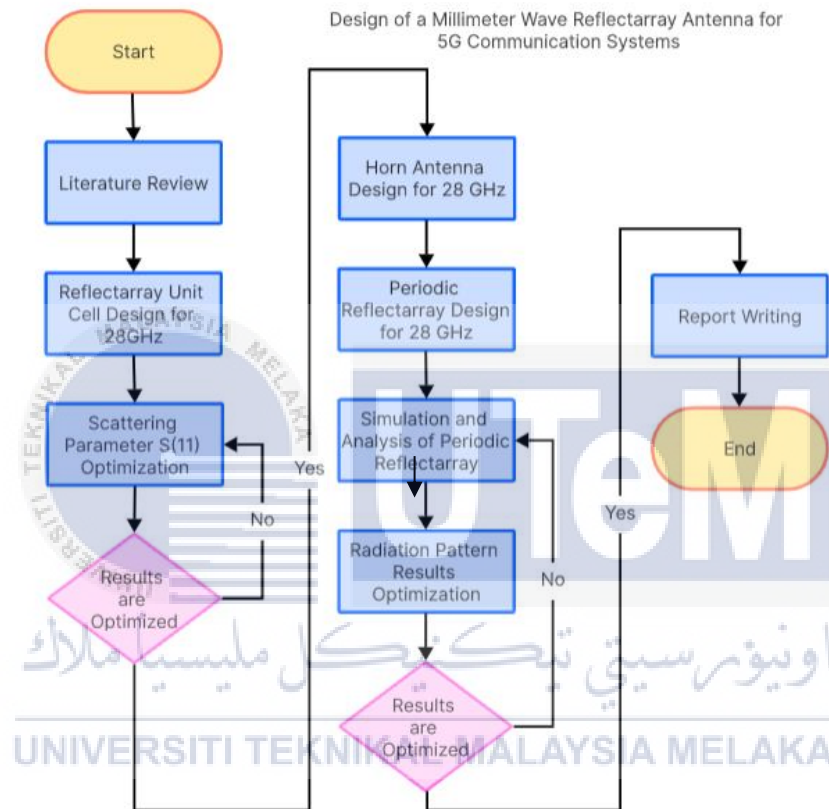


Figure 3.1 Process flow of the project

### 3.4 Experimental Setup

#### 3.4.1 CST Microwave Studio (CST MWS)

CST Microwave Studio (CST MWS) is a specialized software developed by Computer Simulation Technology (CST) that allows engineers and researchers to design and analyze high-frequency electronic devices, antennas, and systems. It utilizes the finite integration technique (FIT) to solve Maxwell's equations numerically and accurately

simulate electromagnetic fields. With a user-friendly interface and powerful solver engine, CST MWS offers a comprehensive toolset for modeling various components, such as antennas, filters, waveguides, and PCBs, by representing their geometry, material properties, and electrical behavior. The software enables users to conduct time-domain and frequency-domain simulations, eigenmode analysis, parametric sweeps, and optimization to evaluate design performance, extract S-parameters, radiation patterns, and impedance matching. Post-processing features allow for visualization and analysis of simulation results, including 2D/3D plots, field animations, and radiation patterns. CST MWS is widely used in antenna design, microwave engineering, RF circuit design, and high-frequency electronics for its advanced capabilities[16].

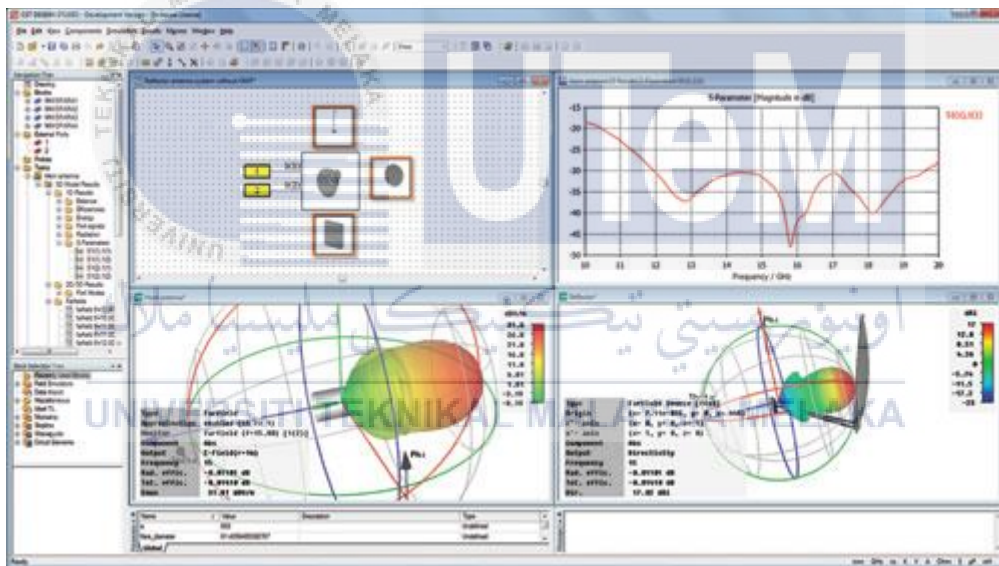


Figure 3.2 Example image of CST MWS project design

### 3.4.2 Scattering Parameter (S11)

The scattering parameter S11 is of utmost importance in CST Microwave Studio (CST MWS) as it serves as a key metric for analyzing the reflection properties of a structure or component. By understanding the S11 parameter, one can evaluate impedance matching, reflection, and performance. In CST MWS, obtaining the S11 parameter involves creating

the geometry, defining boundary conditions, setting up the excitation, running the simulation, and using post-processing tools for result analysis. Analyzing the S11 parameter provides valuable insights into the reflective characteristics of the structure, aiding in the design and optimization of components and evaluating system performance. A comprehensive understanding of the S11 parameter in CST MWS contributes significantly to the development and assessment of electromagnetic systems[17].

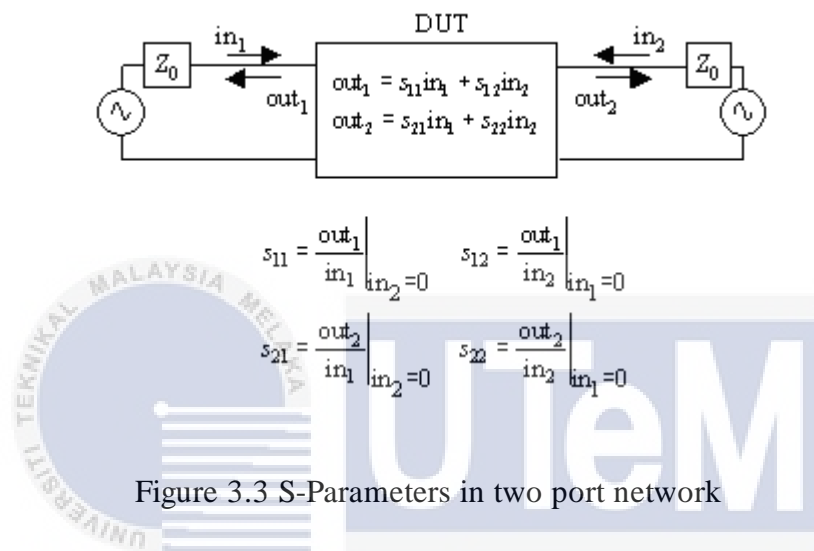


Figure 3.3 S-Parameters in two port network

### 3.4.3 Far-field Radiation Pattern

The far-field radiation pattern is an essential concept in the field of antenna engineering, providing valuable insights into how antennas distribute electromagnetic energy in space. It depicts the spatial arrangement of the radiated power as a function of direction in the far-field region, where the distance from the antenna is sufficient for the pattern to be independent of distance. The far-field radiation pattern offers crucial information about an antenna's directional characteristics, including its gain, beamwidth, directivity, and sidelobe levels.

Within CST Microwave Studio (CST MWS), engineers can utilize electromagnetic simulations and post-processing analysis to obtain the far-field radiation pattern. By defining the antenna's geometry, setting appropriate boundary conditions, and specifying the

excitation source, users can simulate and assess the antenna's radiation behavior. CST MWS facilitates visualizing and analyzing the far-field radiation pattern, empowering engineers to evaluate performance, make necessary adjustments, and optimize the antenna's design.

Optimizing the far-field radiation pattern holds great significance in antenna design, as it governs energy radiation and interaction with the surrounding environment. By leveraging CST MWS to explore the far-field radiation pattern, engineers can evaluate coverage, assess radiation efficiency, identify potential interference or sidelobe concerns, and ensure alignment with specific application requirements. This understanding and optimization of the far-field radiation pattern using CST MWS empower engineers to design antennas that meet performance criteria and enhance system effectiveness in diverse applications like wireless communication, radar systems, and satellite communication [18].

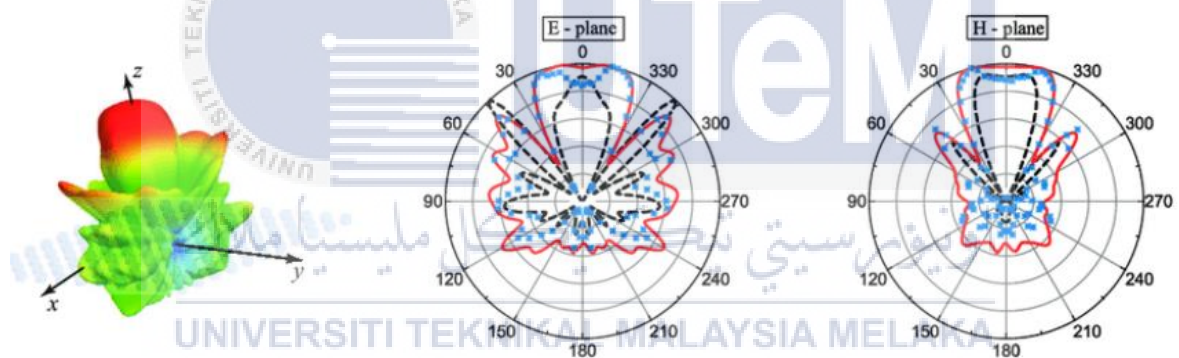


Figure 3.4 The far-field radiation patterns, along with their cross-sectional views in the E-plane and H-plane, are examined.

### 3.5 Summary

The methodology for creating a millimeter wave reflectarray antenna for 5G communication systems involves employing CST MWS software to design and simulate the antenna. A step-by-step flowchart is followed during the design process. Experimental analysis includes assessing the scattering parameter  $S_{11}$  to evaluate reflection properties and impedance matching. Far-field radiation patterns are analyzed to understand how the antenna radiates in different directions and distributes waves. The goal of this methodology is to enhance the antenna's performance for 5G communication systems.



## CHAPTER 4

### RESULTS AND DISCUSSIONS

#### 4.1 Introduction

Chapter 4 presents the results and discussions of the design of a millimeter wave reflectarray antenna for 5G communication systems using CST MWS software. The results include the scattering parameter S11 and far-field radiation patterns. The discussions critically evaluate the obtained results, compare them with desired specifications, and explore potential optimizations. The chapter aims to assess the antenna's performance and provide insights for future advancements in antenna design for wireless communication technologies.

#### 4.2 Results and Analysis

##### 4.2.1 Calculations

The reflectarray unit cell antenna design method required the use of particular calculations based on formulas taken from the antenna book. Below are the fundamental calculations involved in designing the antenna[19].

$$W = \frac{c}{2f_0 \sqrt{\left(\frac{\epsilon R + 1}{2}\right)}}$$
$$\epsilon_{eff} = \frac{\epsilon R + 1}{2} + \frac{\epsilon R - 1}{2} \left[ \frac{1}{\sqrt{\left(1 + 12 \frac{h}{w}\right)}} \right]$$
$$L_{eff} = \frac{c}{2f_0 \sqrt{\epsilon_{eff}}}$$

$$\Delta L = 0.412h \frac{(\epsilon_{eff} + 0.3)\left(\frac{W}{h} + 0.264\right)}{(\epsilon_{eff} - 0.258)\left(\frac{W}{h} + 0.8\right)}$$

$$L = L_{eff} - 2\Delta L$$

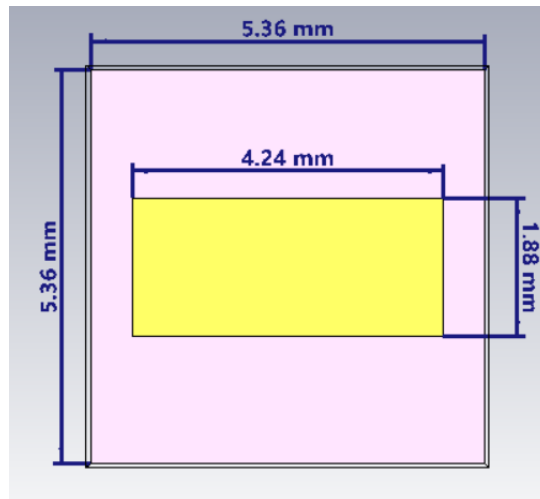
**Where:**

- W = width of the microstrip patch antenna
- L = length of the microstrip patch antenna
- $\epsilon_r$  = dielectric constant
- $f_0$  = resonance frequency
- h = thickness
- c = speed of light

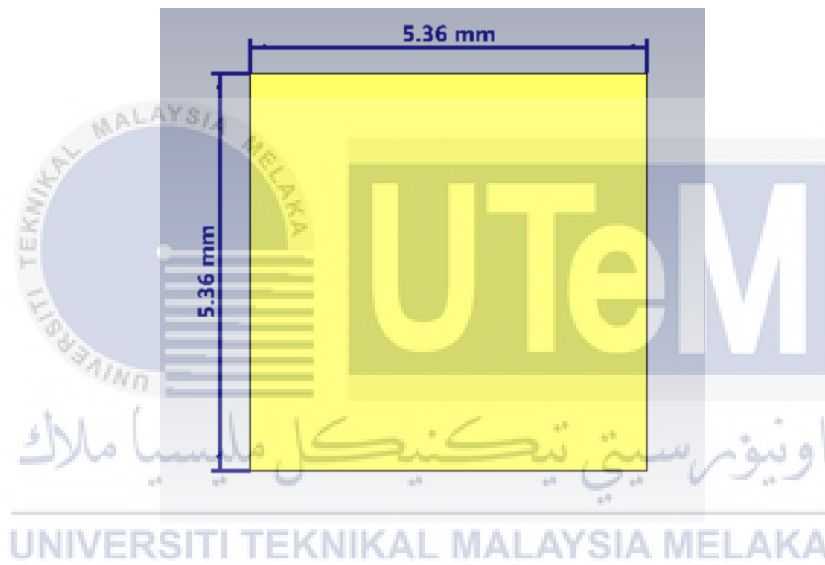
## 4.2.2 Design procedure

### 4.2.2.1 Unit Cell Design

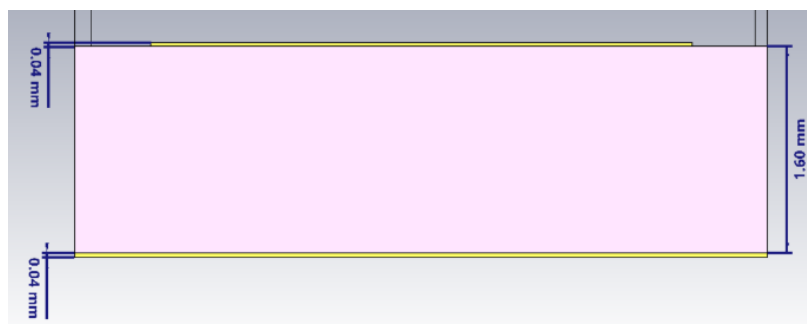
Figures 4.1 depict simulated front, back, and bottom views of the reflectarray unit cell antenna for this project, including its dimensions. In Figure 4.1(a), the substrate and patch widths measure 5.36mm and 4.24mm, while the substrate and patch lengths are 5.36mm and 1.88mm, respectively. In Figure 4.1(b), representing the ground antenna design, the length and width dimensions match those of the substrate, both measuring 5.36mm. The height of the patch and ground is 0.035mm. Figure 4.2 and Figure 4.3 show the parameter list and boundary conditions of the reflectarray unit cell antenna design. Boundary conditions in a unit cell are applied to ensure the accuracy of electromagnetic simulations, particularly in periodic structures. They enable the modeling of the unit cell's interaction with neighboring cells, help study reflection and transmission properties, and play a crucial role in obtaining meaningful results for the overall periodic structure.



(a) Front view



(b) Back view



(c) Side view

Figure 4.1 (a) Front view, (b) Back view, and (c) Bottom view of the unit cell design with dimensions for the length, width, and height of substrate, ground, and patch.

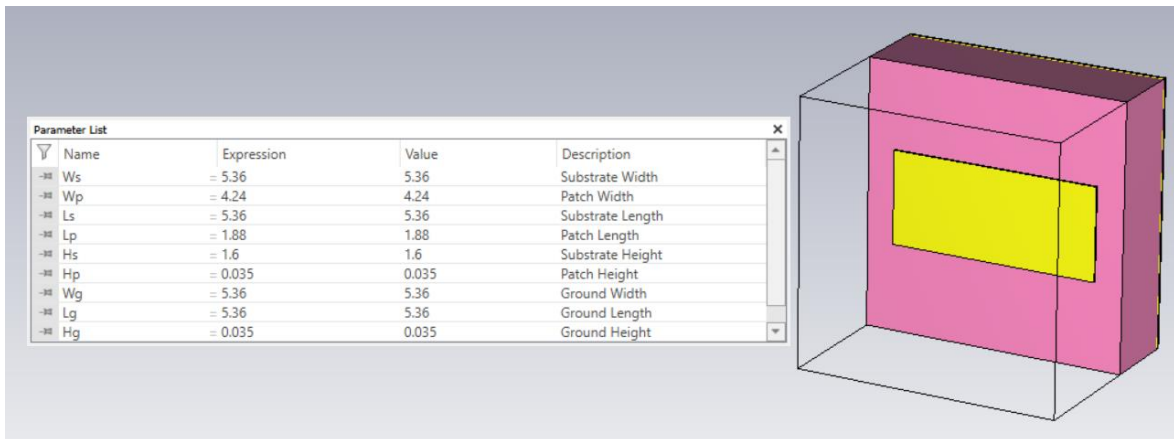


Figure 4.2 Parameter list of unit cell design

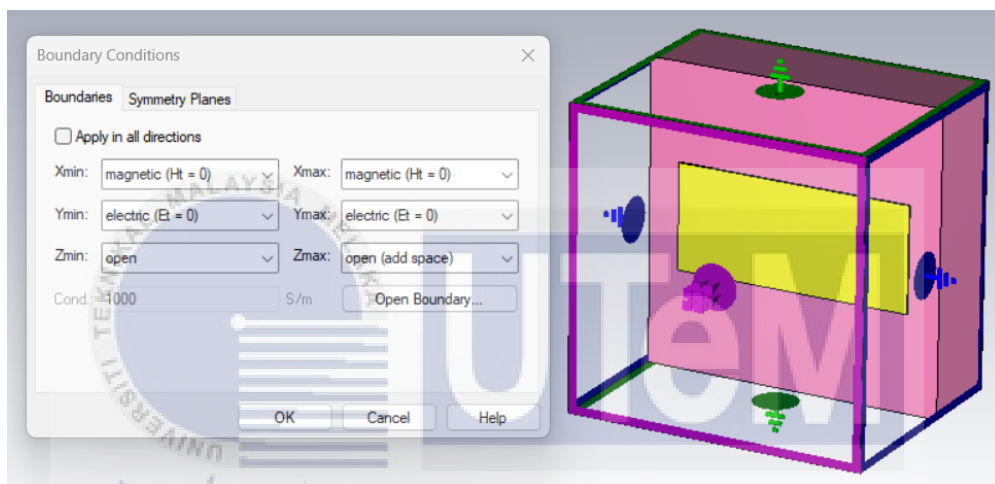


Figure 4.3 Boundary Conditions

#### 4.2.2.2 Horn Antenna Design

Figure 4.4 depicts the design of a horn antenna constructed in CST software. Figure 4.5 illustrates the parameter list essential for designing the horn antenna in the simulation. To construct the horn antenna, it is imperative to assign appropriate values to each parameter. Employing calculated values for these parameters ensures the accuracy and efficacy of the horn antenna design.

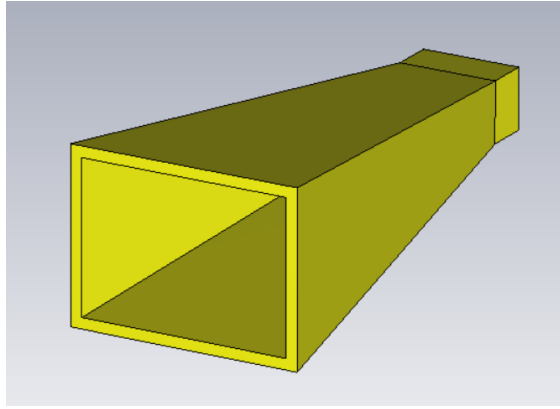


Figure 4.4 Horn antenna design

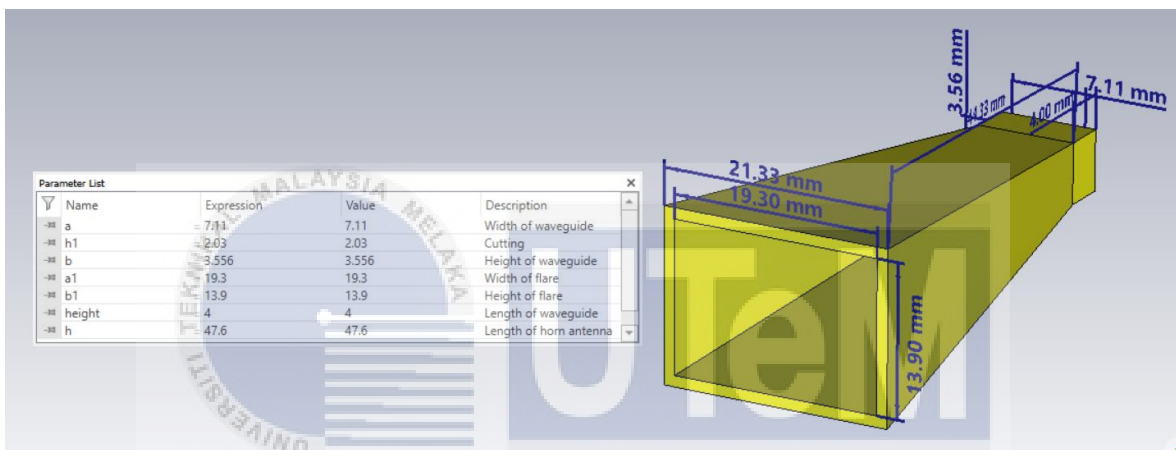


Figure 4.5 Parameter list with dimensions of horn antenna

#### 4.2.2.3 10x10 Reflectarray Design

To design the 10x10 reflectarray antenna in CST simulation, begin by creating the lines and circles on the substrate from curves, following the configuration depicted in Figure 4.6. Subsequently, design the patches one by one on the substrate, starting from the center and progressing towards the right side. The initial five patches differ in length. Once all patches are inserted and translated onto the array, the resulting configuration should resemble the one shown in Figure 4.7, with substrate dimensions of length and width as 53.55x53.55 mm. In Figure 4.8, the parameter list utilized for the design of the 10x10 reflectarray antenna is presented, along with the resulting design of the reflectarray antenna.

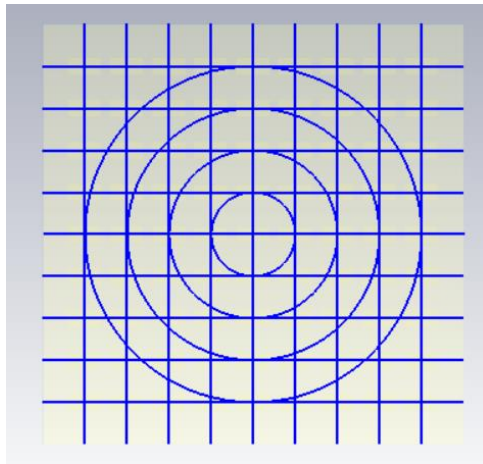


Figure 4.6 Lines and circles from curves

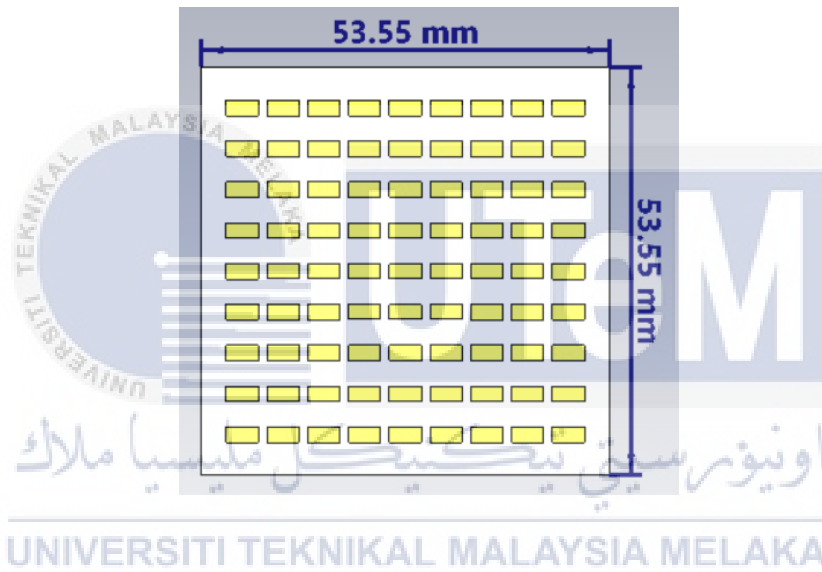


Figure 4.7 10x10 reflectarray design with dimensions

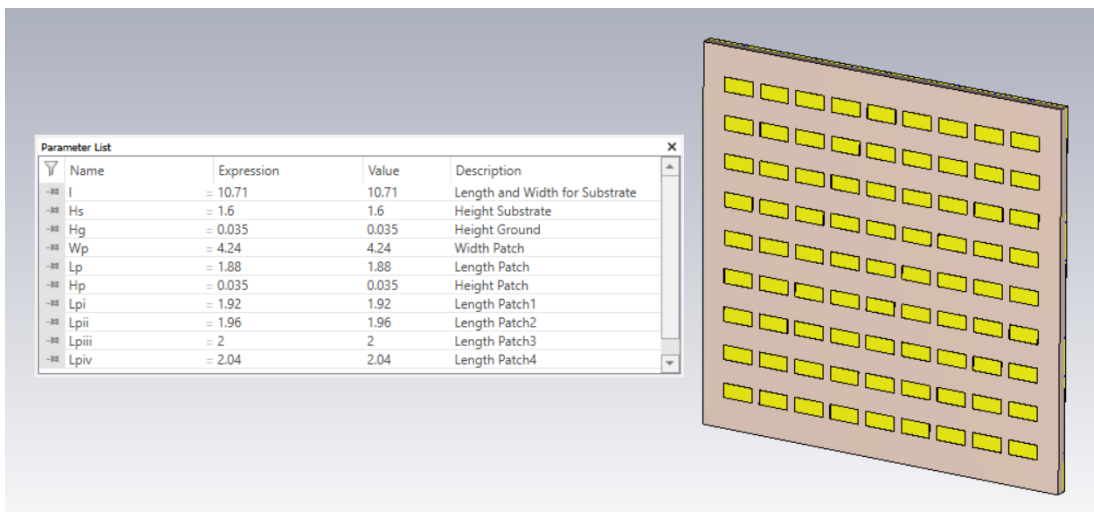


Figure 4.8 Parameter list of 10x10 reflectarray design

#### 4.2.2.4 10x10 Reflectarray Antenna with Horn Antenna Design

In Figure 4.9, the design of the 10x10 reflectarray antenna is depicted, integrated with the horn antenna within the same simulation. To achieve this, begin by copying the horn antenna and pasting it onto the reflectarray antenna. Subsequently, perform a rotation and translation of the horn antenna by specifying the measurement equivalent to the sum of the length of the substrate and the length of the horn antenna in the translating vector Z. This ensures the correct positioning of the horn antenna within the simulation.

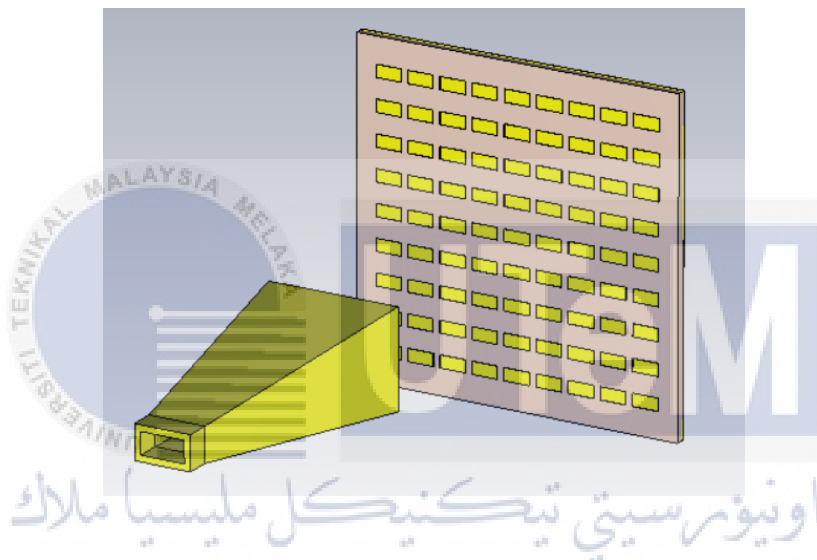


Figure 4.9 Design of the 10x10 reflectarray antenna with horn antenna

#### 4.2.2.5 20x20 Reflectarray Antenna Design

Similar to the previous design of the 10x10 reflectarray antenna, the process for designing a 20x20 reflectarray antenna in CST simulation begins with the creation of lines and circles on the substrate from curves, following the configuration shown in Figure 4.10. Subsequently, design the patches individually on the substrate, starting from the center and extending towards the right side. The initial ten patches have varying lengths. After inserting and translating all patches onto the array, the resulting configuration should resemble the one depicted in Figure 4.11, with substrate dimensions of length and width as 107.1x107.1

mm. Figure 4.12 displays the parameter list employed for the design of the 20x20 reflectarray antenna, along with the resulting antenna design.

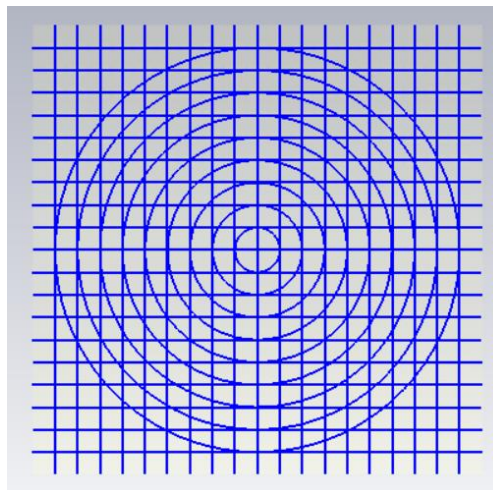


Figure 4.10 Lines and circles from curves

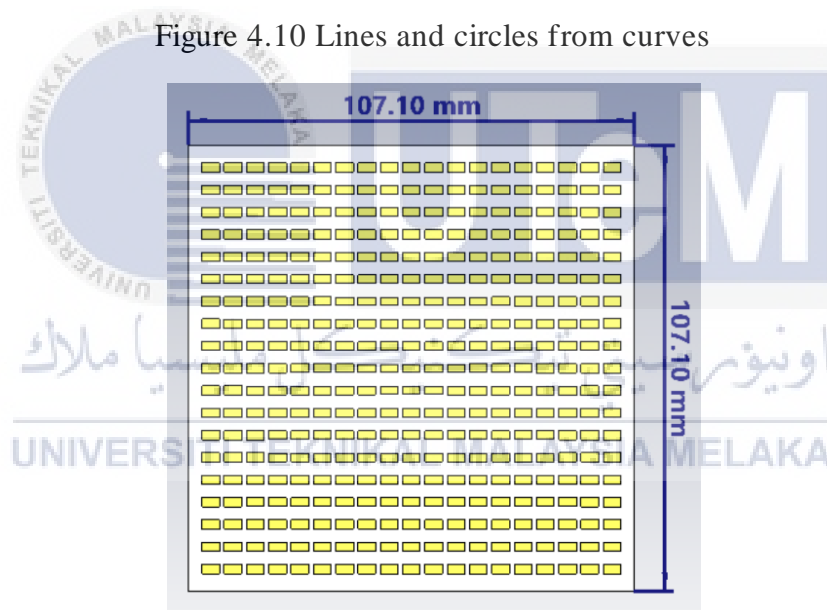


Figure 4.11 20x20 reflectarray design with dimensions

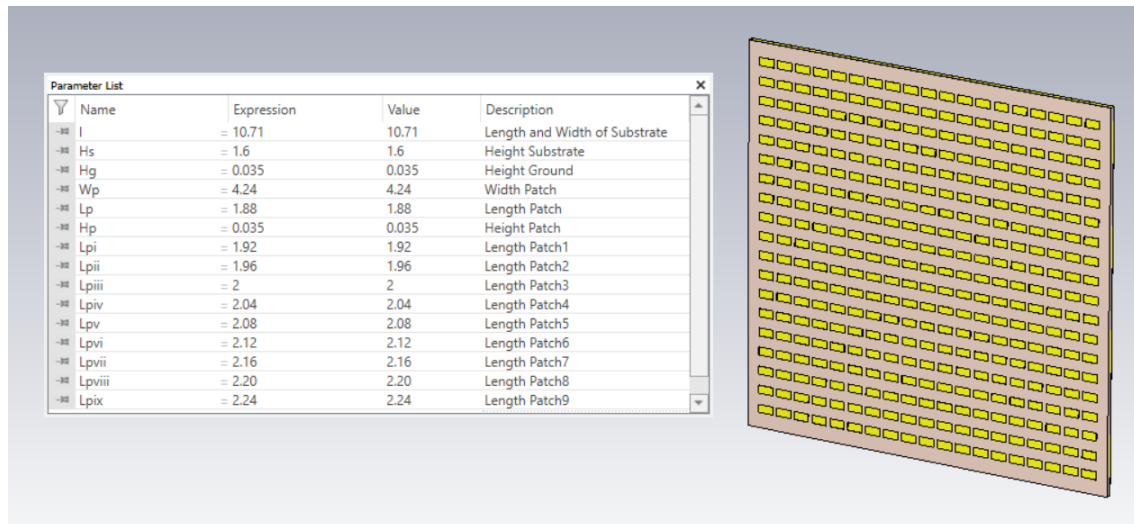


Figure 4.12 Parameter list of 20x20 reflectarray design

#### 4.2.2.6 20x20 Reflectarray Antenna with Horn Antenna Design

Similar to the previous 10x10 reflectarray antenna design, Figure 4.13 illustrates the integration of the 20x20 reflectarray antenna with the horn antenna in the same simulation. The process involves copying the horn antenna and pasting it onto the reflectarray antenna. Subsequently, execute a rotation and translation of the horn antenna, specifying measurements equivalent to the sum of the length of the substrate and the length of the horn antenna in the translating vector Z. This ensures the accurate positioning of the horn antenna within the simulation.

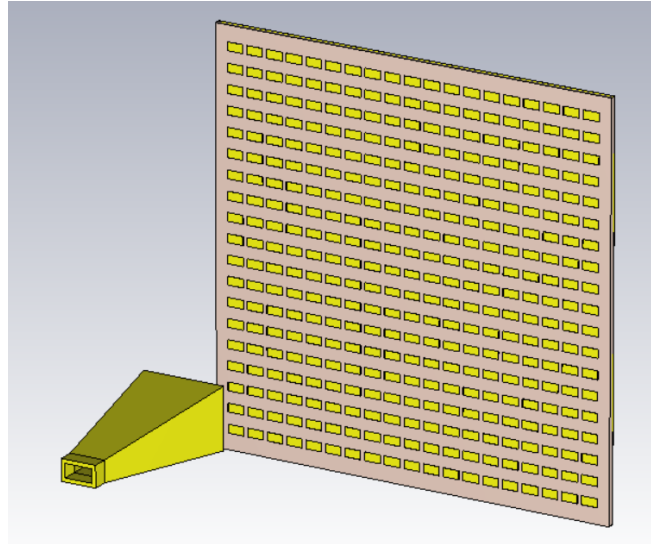


Figure 4.13 Design of the 20x20 reflectarray antenna with horn antenna

#### 4.2.2.7 Fabricated Design of 20x20 Reflectarray

In Figure 4.41, the front and back views of the fabricated design of the 20x20 reflectarray antenna are visually presented, marking a crucial phase in the transition from simulation to physical realization. The fabrication process encompasses several key steps beginning with the preparation of materials, including dielectric substrate material, conductive patches, and a ground plane. Following substrate cleaning, the designed layout is transferred onto the substrate through techniques such as photolithography or direct printing. Notably, the design file from CST software opens on the coral drawing software, facilitating the precise transfer of the reflectarray pattern onto the substrate. The conductive patches are then fabricated with precision, utilizing methods like photolithography, etching, or additive manufacturing. Integration of the ground plane on the back side of the substrate is performed, ensuring proper alignment with the patches on the front side.



Figure 4.14 Front and back view of fabricated design

### 4.2.3 Results and Discussions

The reflectarray unit cell antenna was designed and simulated using CST software, which is capable of analyzing 3D and multilayer configurations. During the simulation, the research recorded the magnitude and phase (in degrees) of the  $S(1,1)$ -parameter.

#### 4.2.3.1 Unit Cell Antenna Design Results

Figure 4.14 illustrates the design of the unit cell with port. In CST software, a “port” is a specified interface on a simulated structure for introducing or extracting electromagnetic signals, crucial for accurately modeling and analyzing devices such as antennas and microwave components. Ports define boundary conditions for signal interaction.

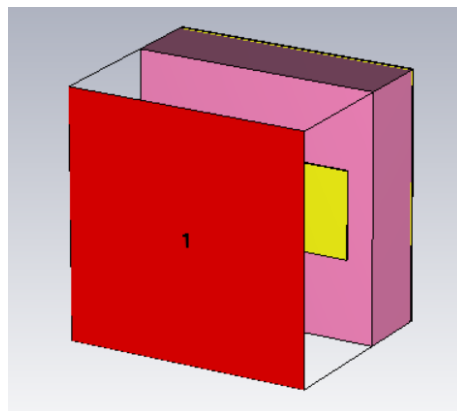


Figure 4.15 Design of the unit cell with port

Next, Figure 4.15 displays the S-Parameter graph for the unit cell design post-simulation. The return loss is measured at -0.0271 dB, occurring at a frequency of 28 GHz. Additionally, the phase, after unwrapping, is recorded at -220.07 degrees at the same frequency, as illustrated in Figure 4.16. These metrics are crucial for evaluating the unit cell's performance in transmitting and reflecting signals at a specific frequency.



Figure 4.16 Graph of S-Parameter for unit cell design

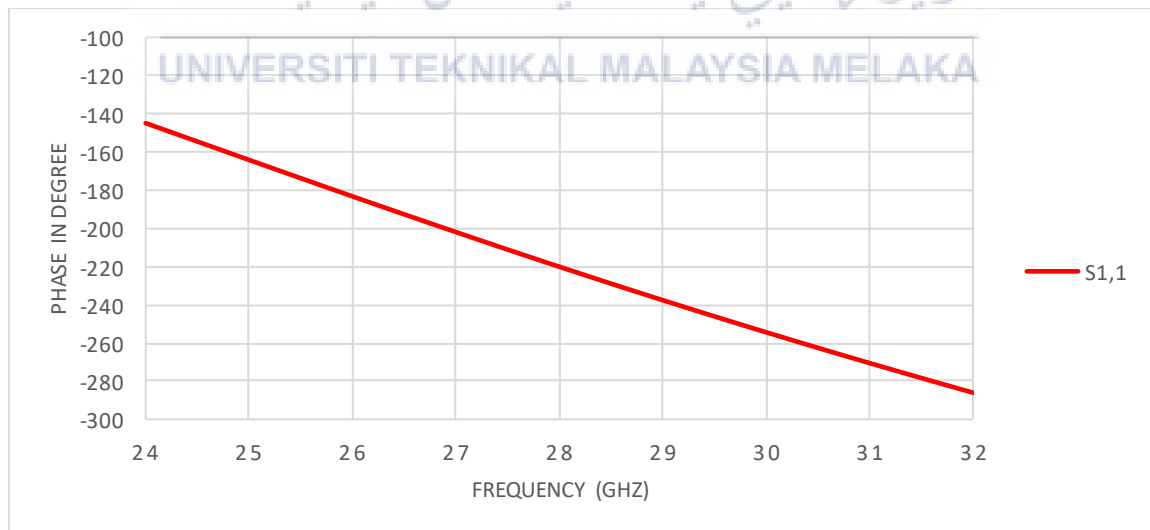


Figure 4.17 Graph of S-Parameter (Phase in Degree) for unit cell design after unwrapped

The parameter sweeps the length of the patch in the range of 1.68 to 2.28 mm with a step width of 0.04 to identify the maximum reflection. The results are presented in Figure 4.17, showcasing the length of the patch where the maximum reflection occurs. It is also similar to Figure 4.18, but it represents the S-parameters for phase after unwrapping in the range of 1.68 to 2.28 mm of the length of the patch. Unwrapping the phase is done to eliminate discontinuities in the phase data, allowing for a continuous and more accurate representation of the signal's progression. This is particularly important in situations where phase information plays a crucial role, such as in the analysis of antennas or RF components.

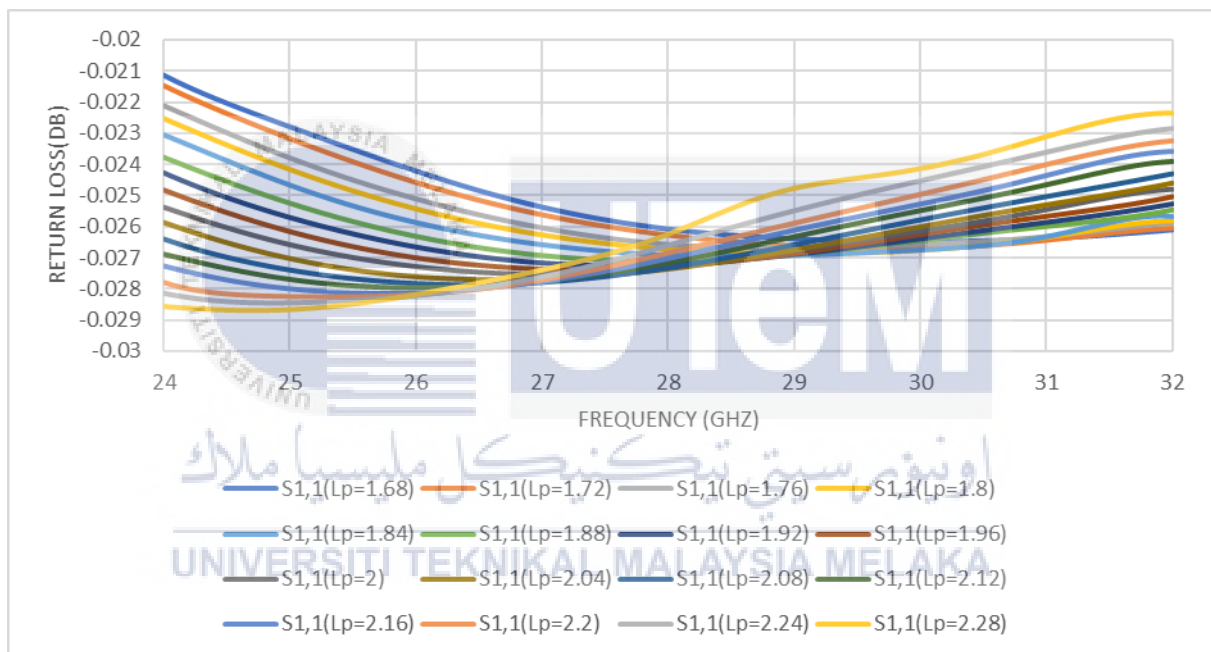


Figure 4.18 Graph of S-Parameter using parameter sweep for different length of patch unit cell

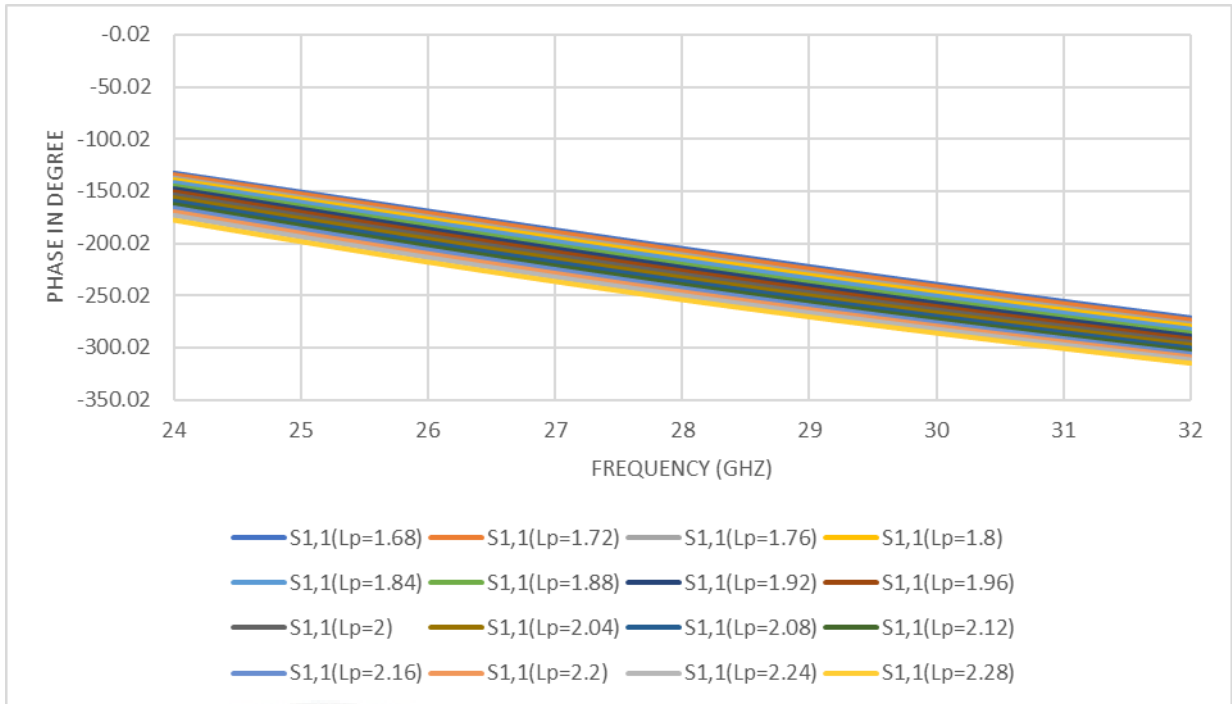


Figure 4.19 Graph of S-Parameter (Phase in Degree) using parameter sweep for different length of patch unit cell after unwrapped

In Figure 4.20, the graph illustrates the relationship between return loss and the length of the patch. It showcases the return loss for each selected length within the earlier specified range. The objective is to identify the optimal length of the patch at 28 GHz for maximum reflection in the periodic array. Similarly, Figure 4.21 presents the phase for each length of the patch. It indicates that as the length of the patch increases, the phase decreases.

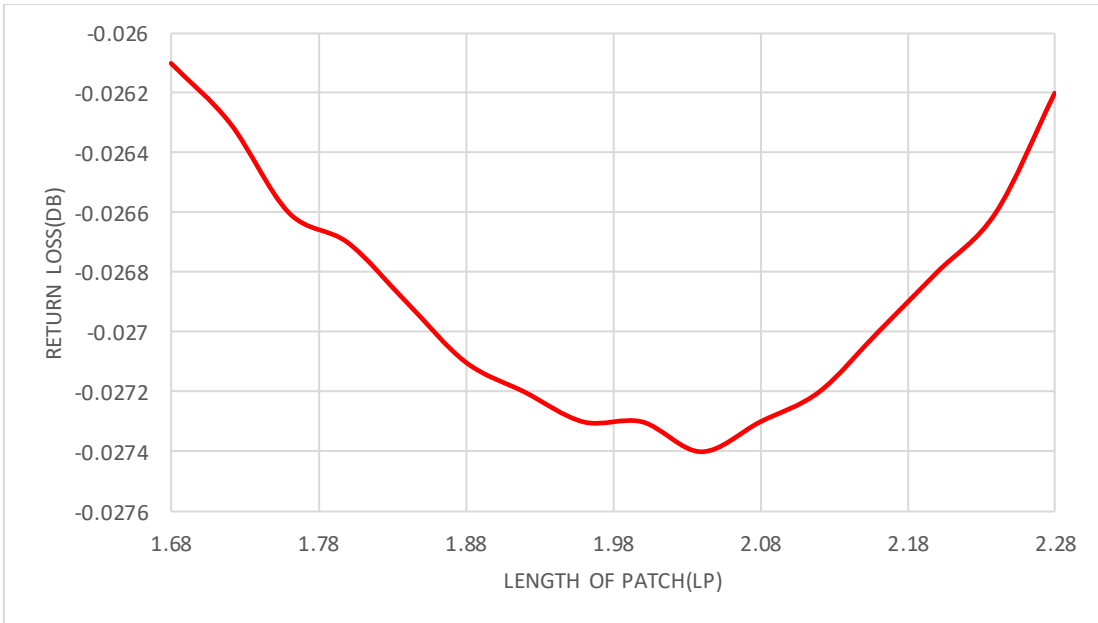


Figure 4.20 Graph of Return Loss VS Length of Patch

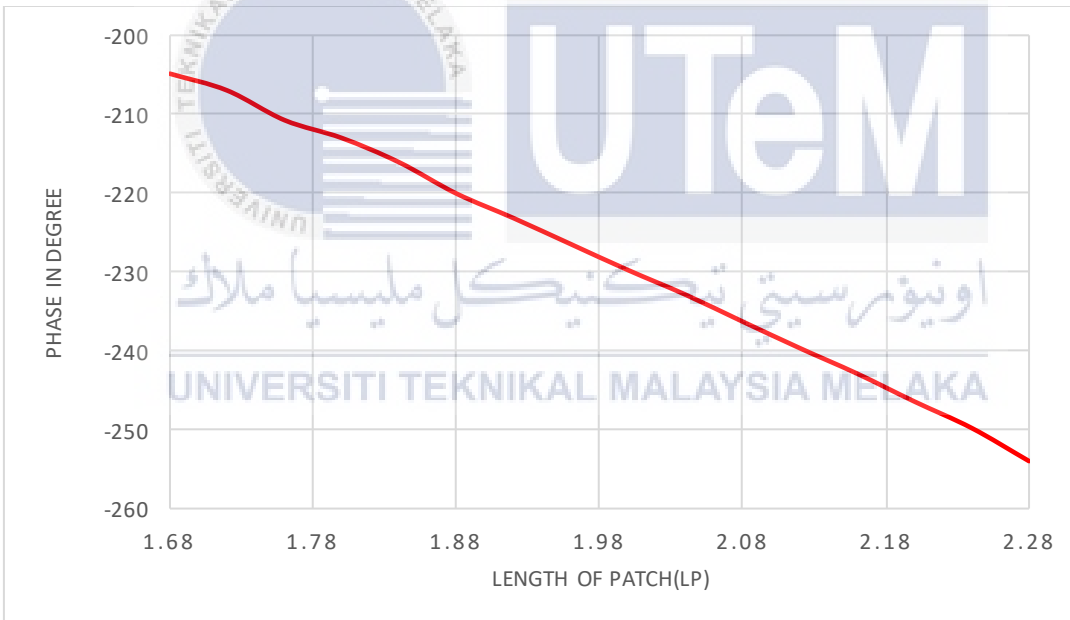


Figure 4.21 Graph of Phase VS Length of Patch

#### 4.2.3.2 Optimization of Horn Antenna

Figure 4.22 depicts the horn antenna design with a port at the back. Following the simulation, the S-parameters in Figure 4.23 reveal a return loss occurring at various

frequencies. Specifically, the horn antenna is designed to transmit a frequency of 28 GHz. The observed return loss is measured at -28.21 dB at this specified frequency.

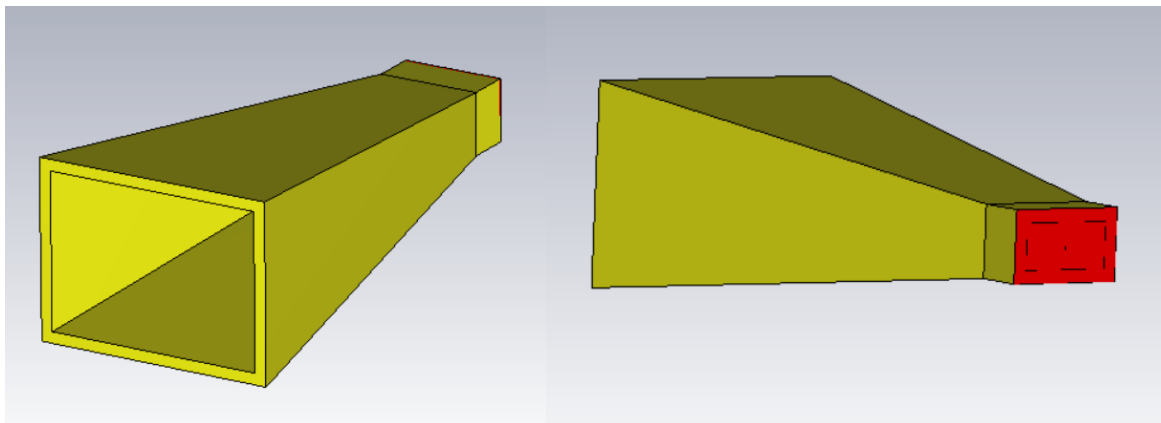


Figure 4.22 Design of the horn antenna with port

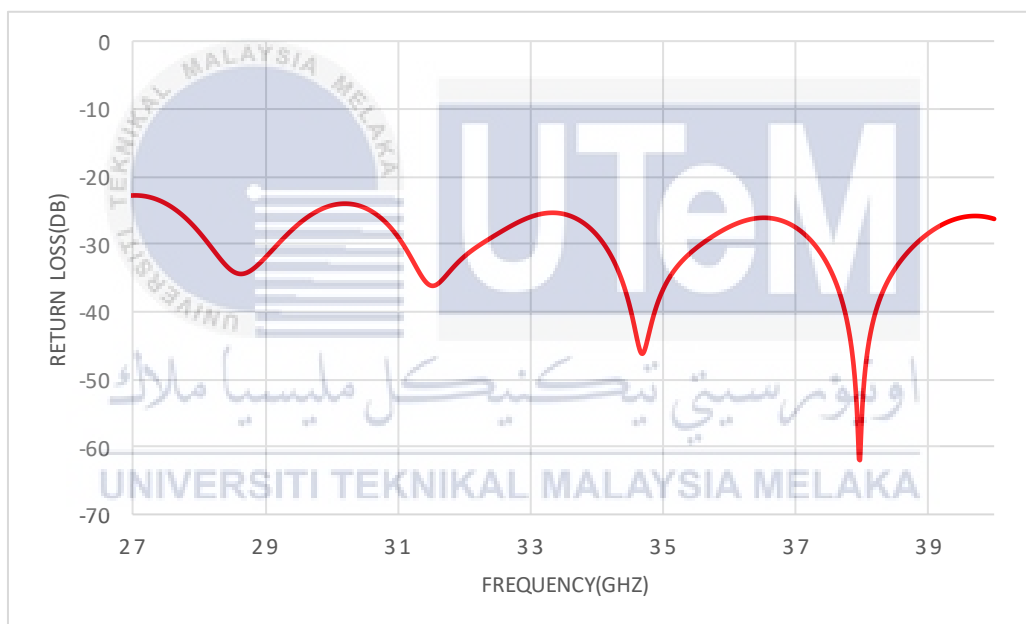


Figure 4.23 Graph of S-Parameter for horn antenna design

#### 4.2.3.3 10x10 Reflectarray Antenna Design Results

In Figure 4.24, the combined design of the 10x10 reflectarray and horn antenna with a port is presented. Subsequently, the S-parameter analysis in Figure 4.25 reveals a return loss of -21.07 dB at a frequency of 28 GHz, indicating the performance of the integrated system.

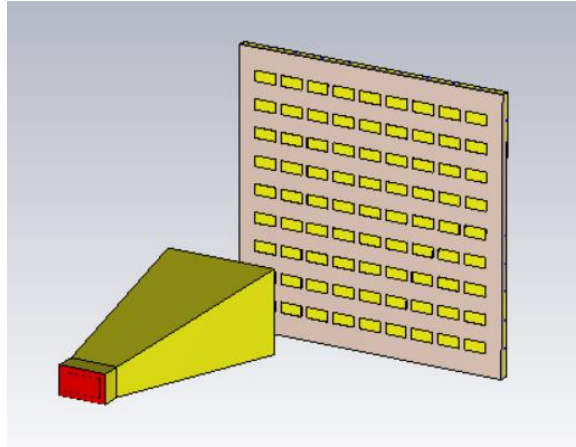


Figure 4.24 Design of the 10x10 reflectarray and horn antenna with port

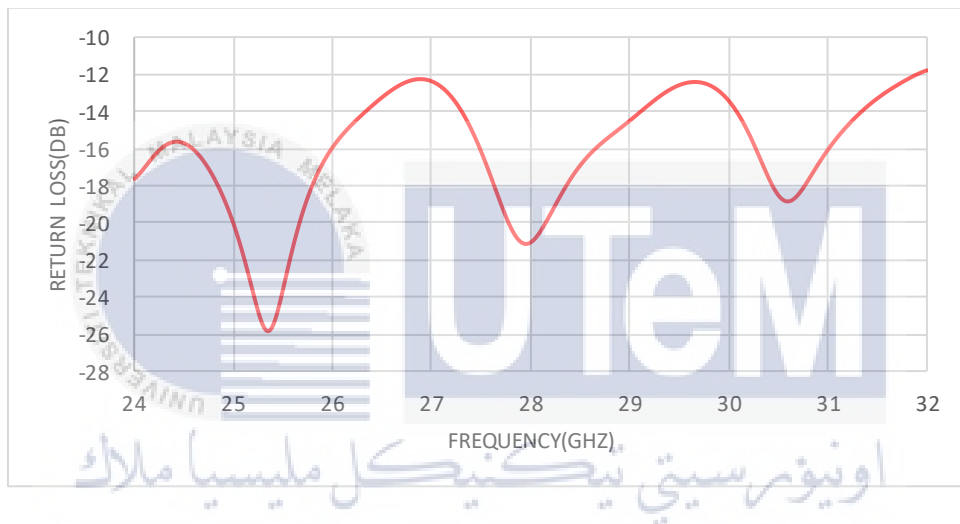


Figure 4.25 Graph of S-Parameter for 10x10 reflectarray antenna design

a) 24GHz

In Figure 4.26, the 2-D and 3-D farfield result for a frequency of 24 GHz is presented. The simulation employs an enabled approximation ( $kR \gg 1$ ) for efficiency. The radiated efficiency is recorded at -0.07292 dB, total efficiency at -0.1480 dB, and the gain is measured at 16.53 dBi. These values characterize the antenna's radiation pattern and effectiveness in transmitting signals in the specified direction at the given frequency.

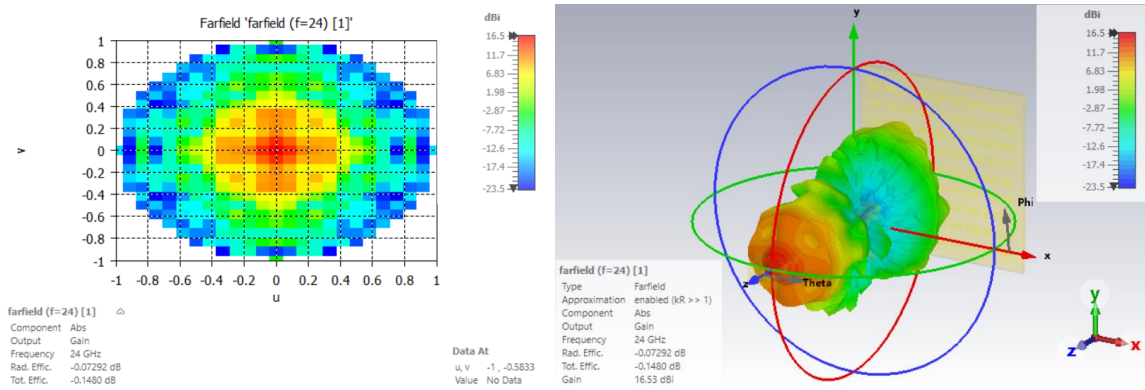


Figure 4.26 2-D and 3-D Farfield gain results for 24GHz

Figure 4.27 illustrates a Cartesian graph of the farfield gain for 24 GHz. The main lobe magnitude is recorded at 16.5 dBi, with a main lobe direction of 0.0 degrees. The angular width (3dB) of the main lobe is measured at 13.5 degrees, and the side lobe level is reported as -4.5 dB. This graph provides a visual representation of the farfield gain characteristics, offering insights into the antenna's radiation pattern and directional properties.

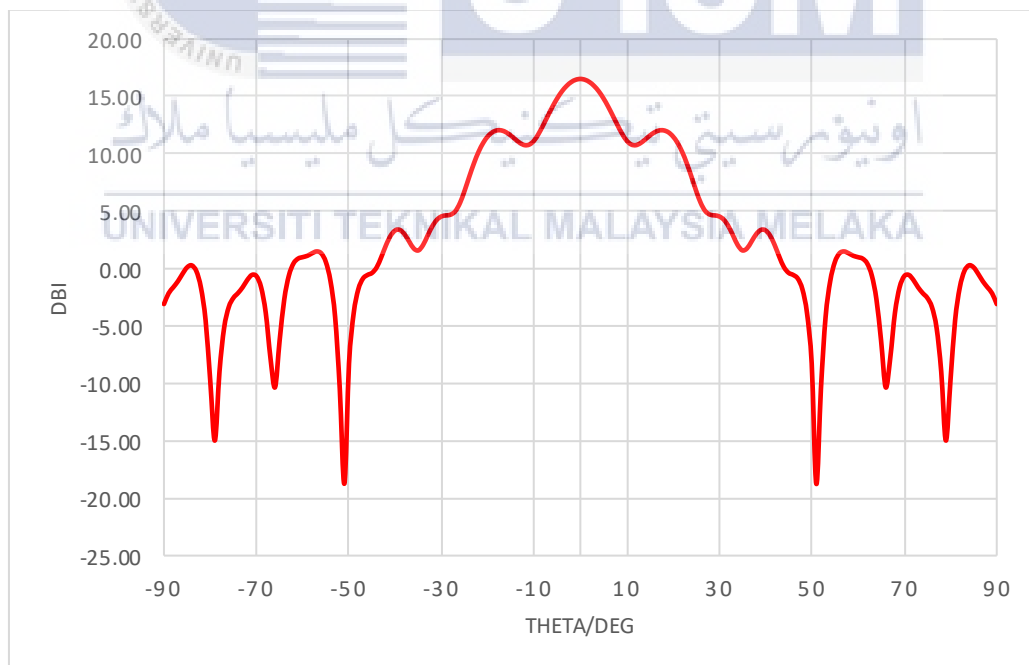


Figure 4.27 Cartesian graph of Farfield gain for 24GHz

b) 28GHz

The 2-D and 3-D farfield results at a frequency of 28 GHz are presented in Figure 4.28. The simulation utilized the 'Farfield' type with an enabled approximation ( $kR \gg 1$ ), focusing on the absolute component and outputting gain. At 28 GHz, the radiation efficiency is reported as -0.06810 dB, total efficiency as -0.1022 dB, and the gain measures 16.88 dBi. These results provide valuable insights into the antenna's directional characteristics and efficiency. Also, Figure 4.29 shows the flow of surface current for the frequency of 28 GHz..

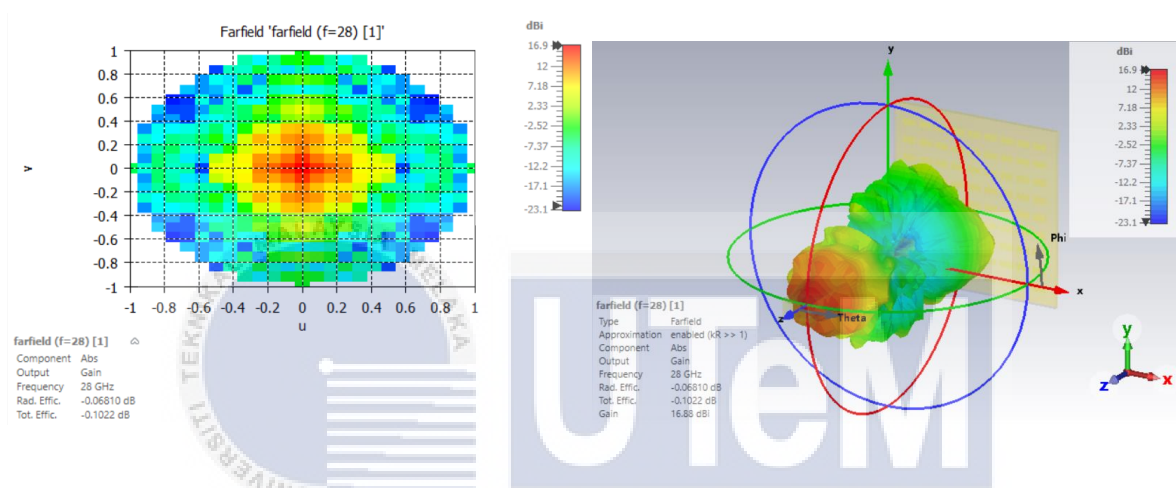


Figure 4.28 2-D and 3-D Farfield gain results for 28GHz

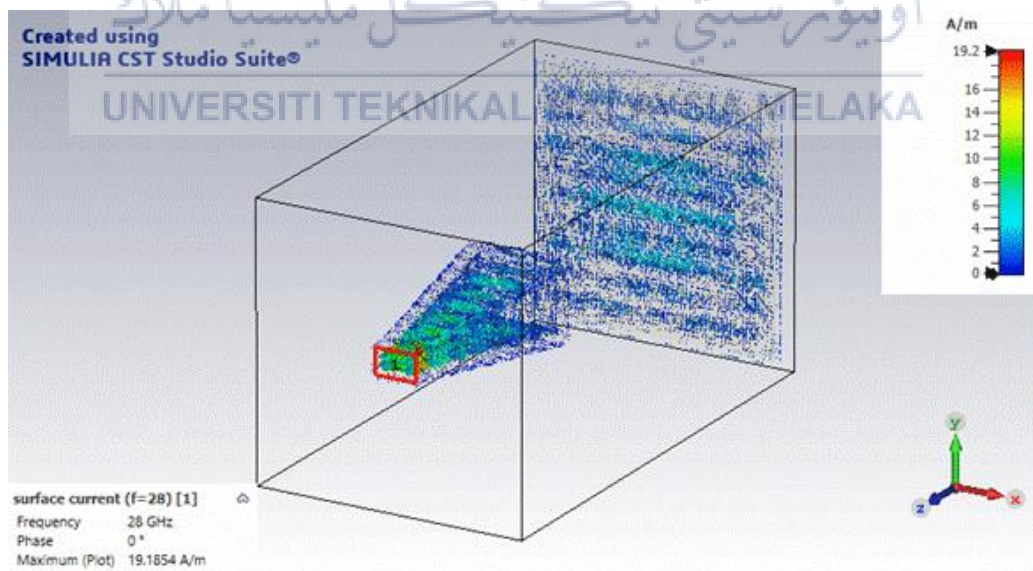


Figure 4.29 Surface current for 28GHz

Figure 4.30 illustrates a Cartesian graph of the Farfield gain for 28 GHz. The main lobe magnitude is measured at 16.9 dBi, with a main lobe direction of 0.0 degrees. The

angular width (3dB) of the main lobe is 13.3 degrees, and the side lobe level is reported as -4.5 dB. These parameters provide a detailed characterization of the antenna's radiation pattern and directional properties.



Figure 4.30 Cartesian graph of Farfield gain for 28GHz

c) 32GHz

In the 2-D and 3-D far-field analysis for a frequency of 32 GHz, as illustrated in Figure 4.31, the 'Farfield' type was employed with an enabled approximation ( $kR \gg 1$ ). The component measured in absolute terms, the output parameter focused on gain, resulting in the following metrics: Radiated Efficiency of -0.03135 dB, Total Efficiency of -0.3285 dB, and a Gain of 17.80 dBi. These values provide a comprehensive understanding of the antenna's radiation characteristics and efficiency at the specified frequency, crucial for evaluating its performance in the designated operational range.

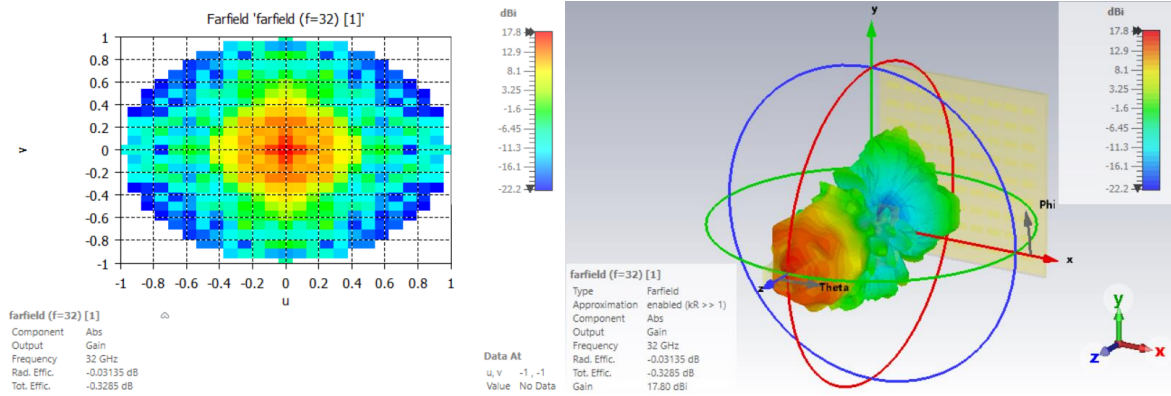


Figure 4.31 2-D and 3-D Farfield gain results for 32GHz

In figure 4.32 displays a Cartesian graph illustrating the Farfield gain for a frequency of 32 GHz. The main lobe magnitude is recorded at 17.8 dBi, with a main lobe direction of 0.0 degrees. The angular width of the main lobe, measured at the 3dB points, is 12.5 degrees. Additionally, the side lobe level is reported as -3.8 dB. These parameters provide a detailed depiction of the antenna's radiation pattern, showcasing its directional characteristics and side lobe levels at the specified frequency.

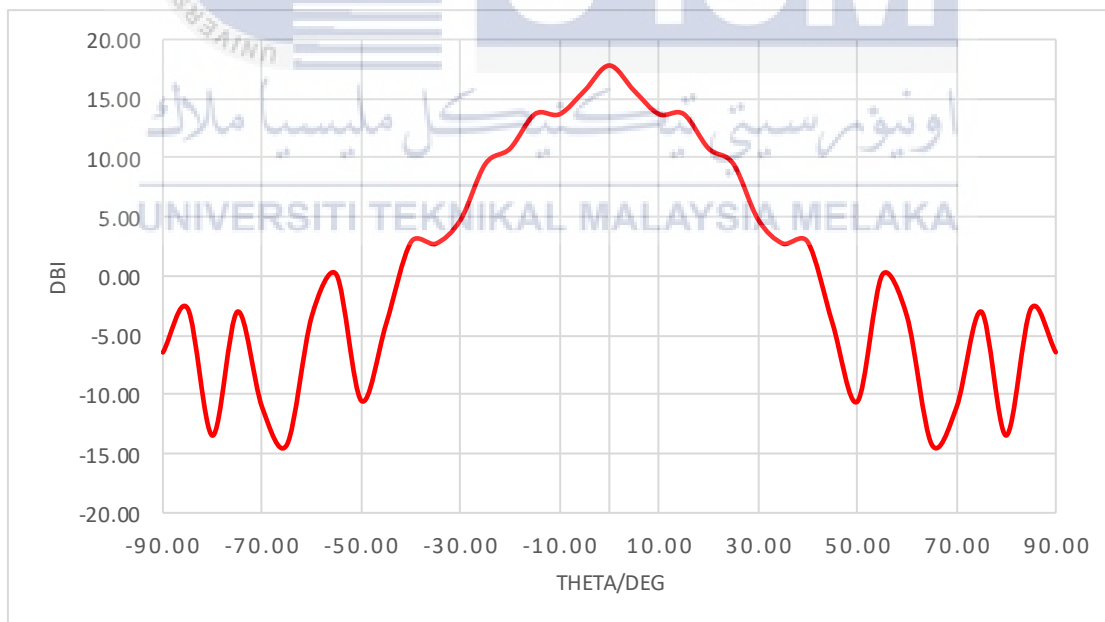


Figure 4.32 Cartesian graph of Farfield gain for 32GHz

d) Maximum Gain Vs Frequency(GHz)

Figure 4.33 presents a plot of Maximum Gain versus Frequency (GHz) for the 10x10 reflectarray antenna design, showcasing the variation in maximum gain across the frequency range of 24 GHz to 32 GHz. The graph highlights that the highest gain is achieved at 29.59 GHz, reaching 18.89 dBi. A comparative analysis at 24 GHz, 28 GHz, and 32 GHz indicates that the maximum gain is 17.8 dBi at 32 GHz. However, it is noteworthy that even at 28 GHz, a significant maximum gain of 16.9 dBi is observed, surpassing the gain at 24 GHz.

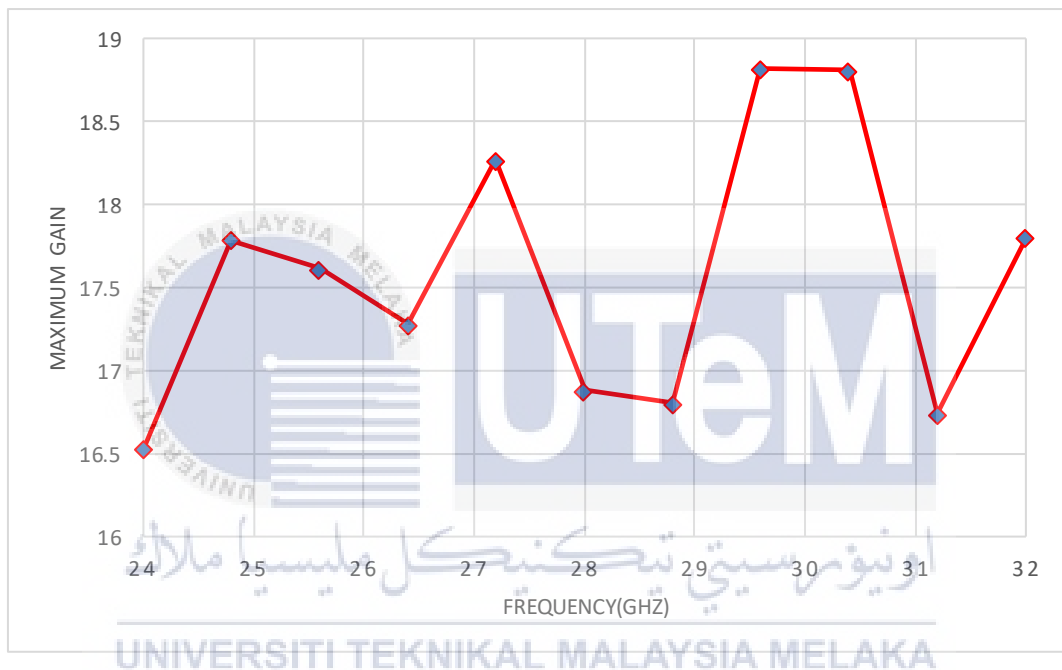


Figure 4.33 Maximum Gain Vs Frequency(GHz) for 10x10 reflectarray antenna design

#### 4.2.3.4 20x20 Reflectarray Antenna Design Results

Similar to the previous design, Figure 4.34 illustrates the integrated design of a 20x20 reflectarray and horn antenna with a port. The subsequent S-parameter analysis in Figure 4.35 demonstrates a return loss of -26.84 dB at a frequency of 28 GHz, providing insights into the performance of the combined system.

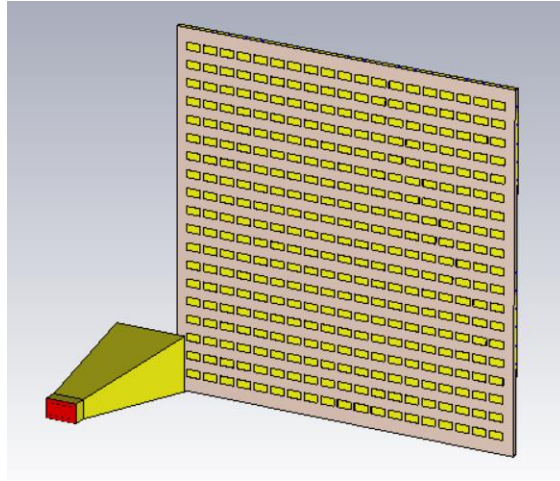


Figure 4.34 Design of the 20x20 reflectarray antenna with port

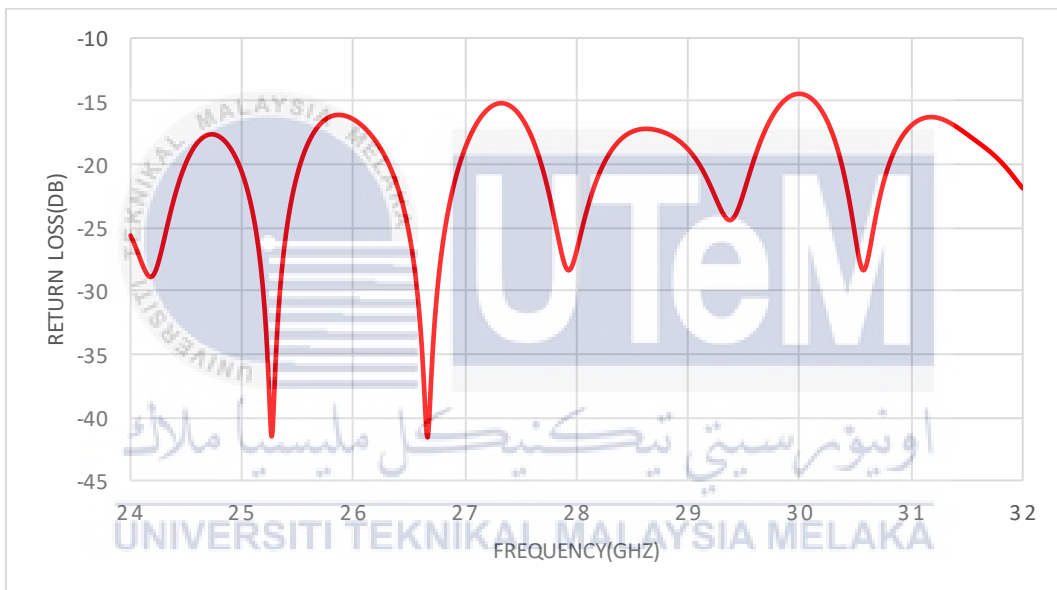


Figure 4.35 Graph of S-Parameter for 20x20 reflectarray antenna design

a) 24GHz

In the analysis of the 2-D and 3-D far-field results for a frequency of 24 GHz, as illustrated in Figure 4.36, the 'Farfield' type was employed with an enabled approximation ( $kR \gg 1$ ). The component measured in absolute terms, and the output parameter focused on gain, resulting in the following metrics: Radiated Efficiency of -0.04051 dB, Total Efficiency of -0.05240 dB, and a Gain of 14.16 dBi. These values offer valuable insights into the radiation characteristics and efficiency of the antenna at the specified frequency, aiding in the assessment of its performance.

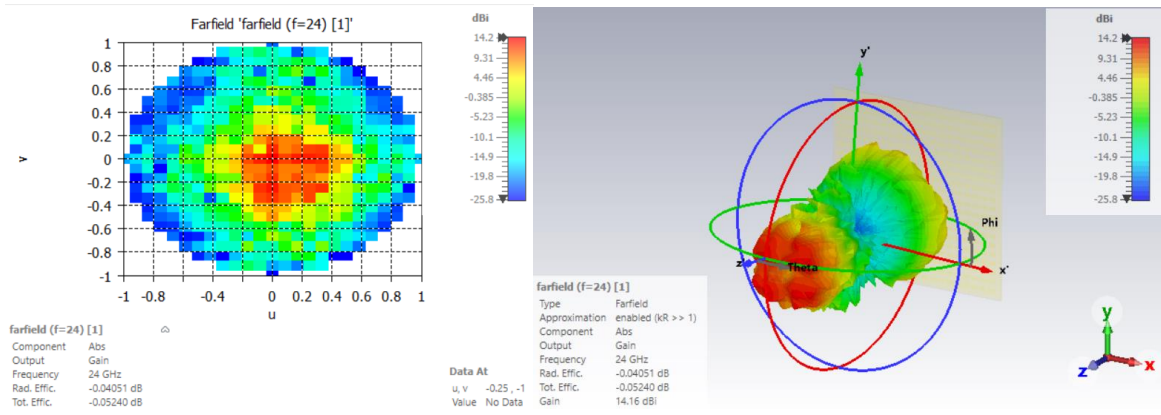


Figure 4.36 2-D and 3-D Farfield gain results for 24GHz

Figure 4.37 exhibits a Cartesian graph illustrating the Farfield gain for a frequency of 24 GHz. The main lobe magnitude is recorded at 14.2 dBi, with a main lobe direction of 0.0 degrees. The angular width of the main lobe, measured at the 3dB points, is 15.0 degrees. Additionally, the side lobe level is reported as -0.7 dB. These parameters offer a detailed representation of the antenna's radiation pattern, highlighting the directional characteristics and side lobe levels at the specified frequency.

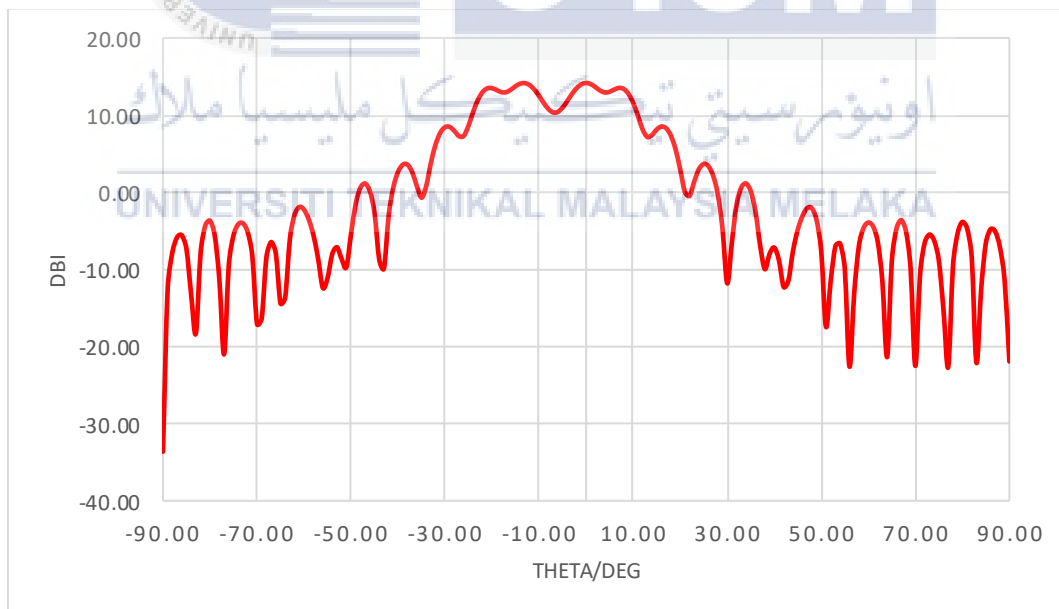


Figure 4.37 Cartesian graph of Farfield gain for 24GHz

b) 28GHz

In the 2-D and 3-D far-field analysis for a frequency of 28 GHz, detailed in Figure 4.38, the 'Farfield' type was employed with an enabled approximation ( $kR \gg 1$ ). The component measured in absolute terms, and the output parameter focused on gain, resulting in the following metrics: Radiated Efficiency of -0.07109 dB, Total Efficiency of -0.08009 dB, and a Gain of 14.96 dBi. These values offer comprehensive insights into the radiation characteristics and efficiency of the antenna system at the specified frequency, critical for assessing its performance in practical applications. Also, Figure 4.39 shows the flow of surface current for a frequency of 28 GHz.

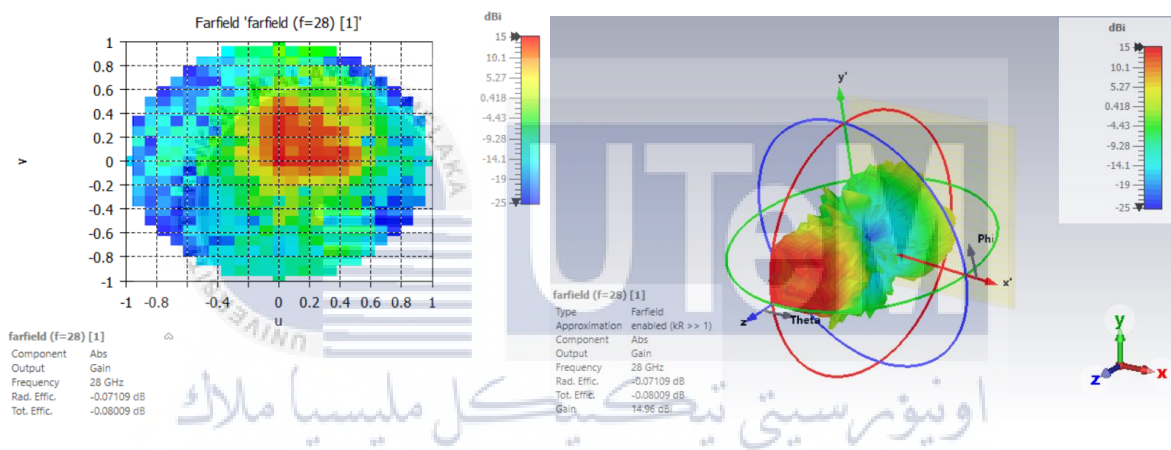


Figure 4.38 2-D and 3-D Farfield gain results for 28GHz

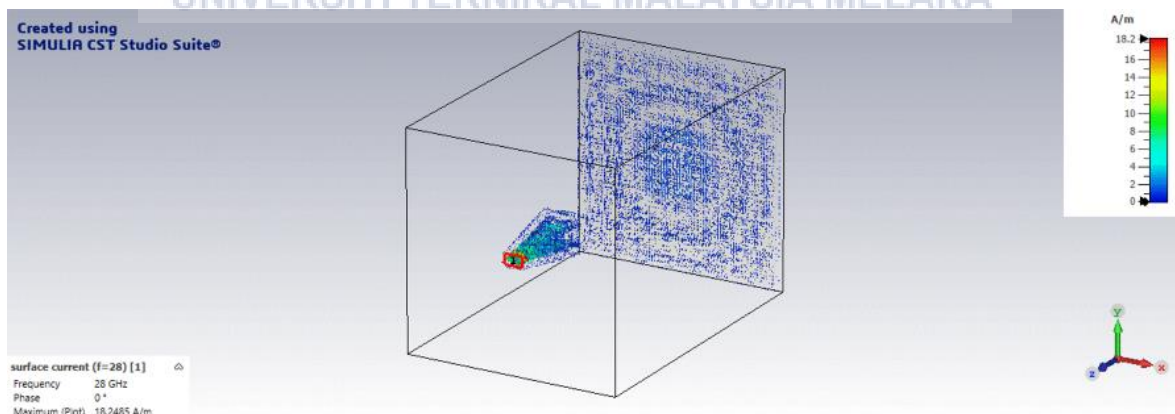


Figure 4.39 Surface current for 28GHz

Figure 4.40 illustrates a Cartesian graph depicting the Farfield gain for a frequency of 28 GHz. The main lobe magnitude is measured at 15 dBi, with a main lobe direction of

0.0 degrees. The angular width, measured at the 3dB points, is 29.1 degrees. Additionally, the side lobe level is reported as -4.7 dB. These parameters offer a detailed characterization of the antenna's radiation pattern, showcasing its main lobe properties and side lobe levels at the specified frequency.

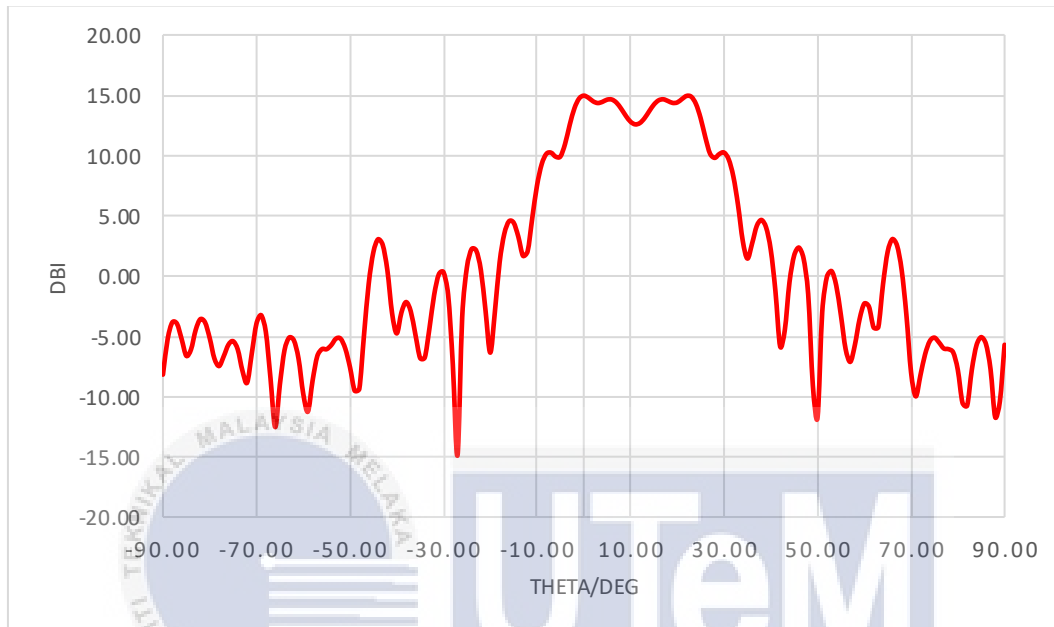


Figure 4.40 Cartesian graph of Farfield gain for 28GHz

c) 32GHz

In the 2-D and 3-D far-field analysis for a frequency of 32 GHz, as depicted in Figure 4.41, the 'Farfield' type was employed with an enabled approximation ( $kR \gg 1$ ). The component measured in absolute terms, with the output parameter focused on gain, resulted in the following metrics: Radiated Efficiency of -0.1086 dB, Total Efficiency of -0.1369 dB, and a Gain of 16.82 dBi. These values offer a comprehensive evaluation of the antenna's radiation characteristics and efficiency at the specified frequency, essential for understanding its performance within the designated frequency range.

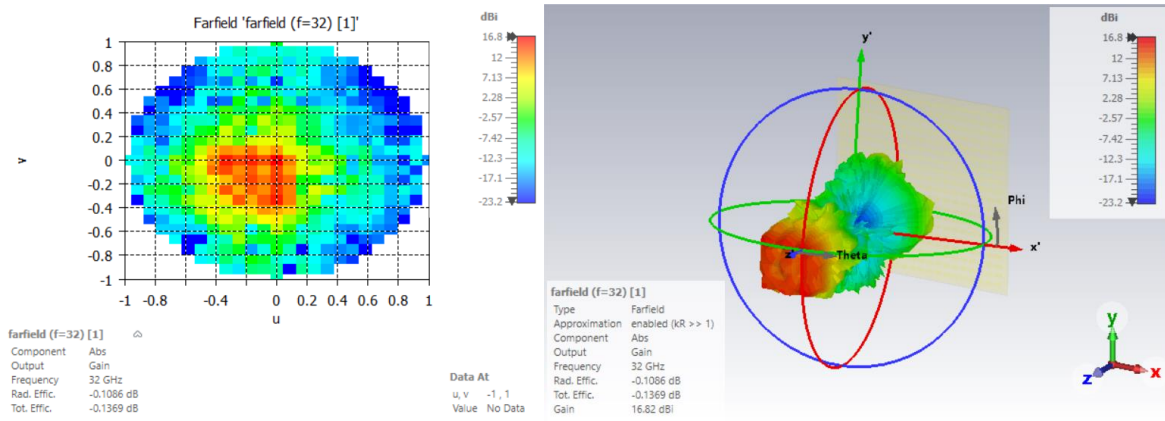


Figure 4.41 2-D and 3-D Farfield gain results for 32GHz

Figure 4.42 presents a Cartesian graph illustrating the Farfield gain for a frequency of 32 GHz. The main lobe magnitude is recorded at 16.8 dBi, with a main lobe direction of 0.0 degrees. The angular width of the main lobe, measured at the 3dB points, is 25.7 degrees. Additionally, the side lobe level is reported as -4.7 dB. These parameters offer detailed insights into the radiation pattern of the antenna, including main lobe characteristics and side lobe levels at the specified frequency.

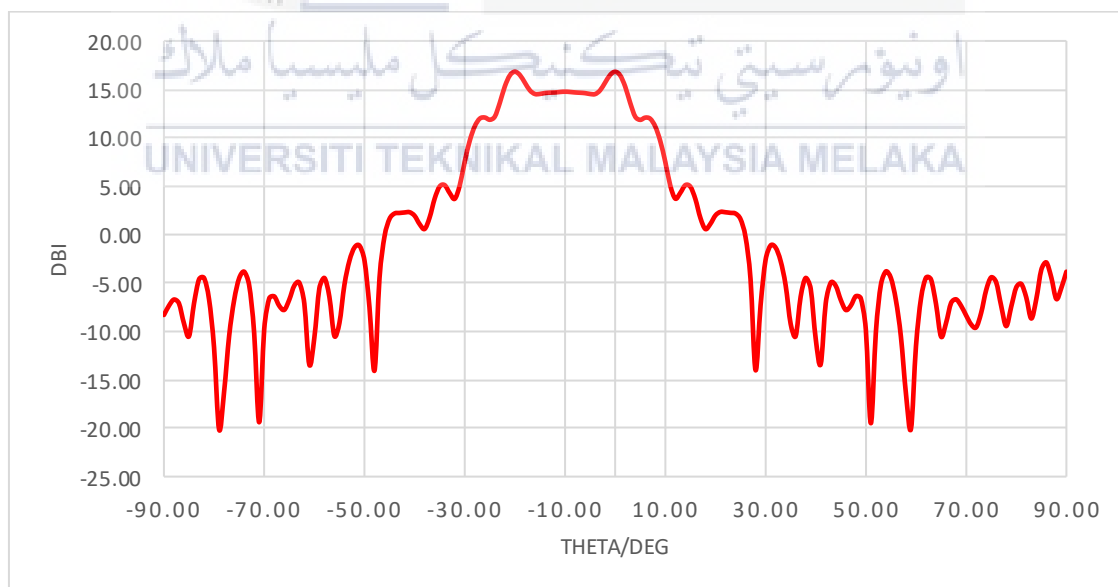


Figure 4.42 Cartesian graph of Farfield gain for 32GHz

d) Maximum Gain Vs Frequency(GHz)

Figure 4.43 illustrates the Maximum Gain versus Frequency (GHz) plot for the 20x20 reflectarray antenna design, providing insights into the gain variation across the frequency range of 24 GHz to 32 GHz. The graph emphasizes the peak gain at 31.19 GHz, registering at 17.02 dBi. Upon further analysis at 24 GHz, 28 GHz, and 32 GHz, the maximum gain is identified as 16.82 dBi at 32 GHz. Notably, at 28 GHz, a substantial maximum gain of 14.96 dBi is observed, surpassing the gain recorded at 24 GHz.

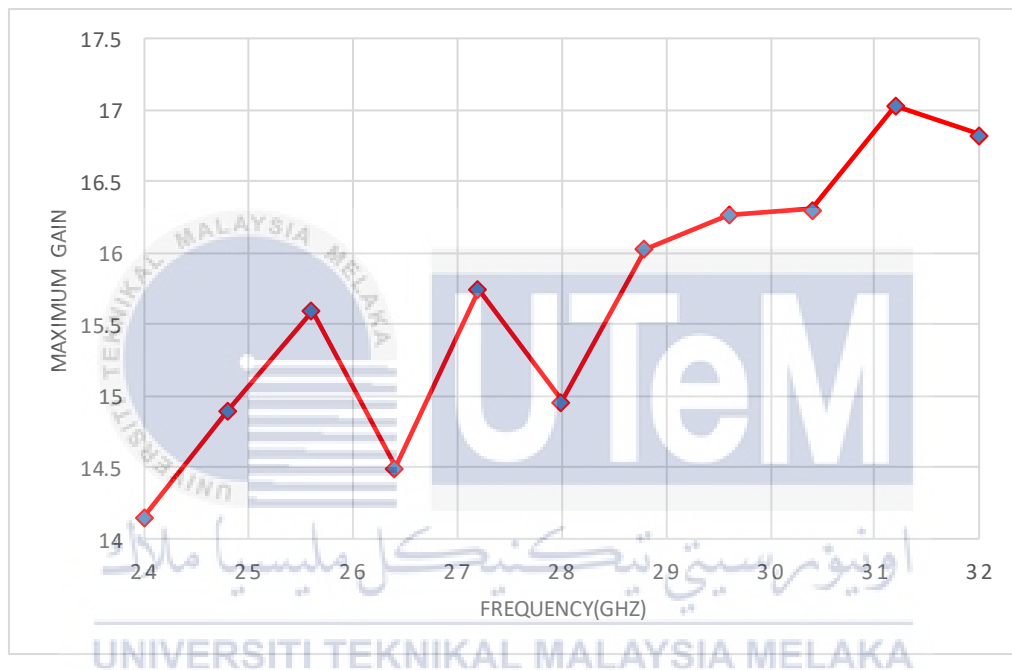


Figure 4.43 Maximum Gain Vs Frequency(GHz) for 10x10 reflectarray antenna design

### 4.3 Summary

Chapter 4 of the document details the design and simulation results of a millimeter-wave reflectarray antenna for 5G communication systems using CST MWS software. The design involves a unit cell antenna, a horn antenna, and 10x10 and 20x20 reflectarray antennas, both with and without an integrated horn antenna. Importantly, the document extends its coverage to include the fabrication process, particularly highlighting the completion of the fabrication for the 20x20 reflectarray design. The chapter provides a step-

by-step explanation of the design process, including calculations and parameter considerations.

For the unit cell antenna, simulations were conducted to analyze S-parameters, with specific attention to return loss and phase. Parameter sweeps were performed to identify optimal patch lengths. The horn antenna and reflectarray antennas were also designed and simulated, with emphasis on S-parameters and far-field radiation patterns at frequencies of 24 GHz, 28 GHz, and 32 GHz. The results include graphs depicting return loss, phase, and far-field gain characteristics.

Key findings include the optimization of patch length for the unit cell antenna, return loss measurements for the horn antenna at 28 GHz, and far-field results for both 10x10 and 20x20 reflectarray antennas. The document concludes with a comprehensive analysis of maximum gain versus frequency for both reflectarray designs. The information presented in Chapter 4 aims to assess the antenna's performance and contribute insights for future advancements in millimeter-wave reflectarray antenna design for 5G communication systems.



## CHAPTER 5

### CONCLUSION AND RECOMMENDATIONS

#### 5.1 Conclusion

In conclusion, this project aimed to address challenges in designing a millimeter-wave reflectarray antenna for 5G communication at 28 GHz, leveraging the capabilities of Computer Simulation Technology (CST) software. The objectives focused on unit cell optimization, periodic reflectarray design, and simulation of radiation properties. Chapter 1 outlined the project scope, emphasizing CST software's crucial role in accurate simulation and optimization, while acknowledging limitations in fabrication, environmental assumptions, and interference neglect.

Chapter 2 provided a comprehensive literature review, exploring recent developments in millimeter-wave reflectarray antennas for 5G. Various studies highlighted the advantages and challenges of designs such as dual-band reflectarrays, compact antenna arrays, and adaptive beamsteering techniques, offering insights into their potential for enhancing 5G communication systems.

Chapter 3 detailed the methodology, emphasizing the use of CST MWS software. The step-by-step flowchart guided the design process, incorporating experimental analysis of S11 parameters and far-field radiation patterns to enhance the antenna's 5G performance.

Chapter 4 presented the core of the project, detailing the design and simulation results of unit cell, horn, and 10x10 and 20x20 reflectarray antennas. Key findings included optimized patch lengths for the unit cell, return loss measurements for the horn antenna, and far-field results for both reflectarrays at different frequencies. Crucially, the document

extended its coverage to include the fabrication process, emphasizing the completion of the fabrication for the 20x20 reflectarray design.

In summary, this project has made significant strides in optimizing millimeter-wave reflectarray antennas for 5G communication, providing valuable insights for future advancements. The combination of simulation results, optimization strategies, and the inclusion of the fabrication process enhances the document's contribution to the field, laying a foundation for further innovation in millimeter-wave reflectarray antenna design.

## 5.2 Future Works

Future work for this project could focus on several areas to further enhance the design and performance of the millimeter wave reflectarray antenna for 5G communication systems. Some potential avenues for future exploration include:

### a) Optimization of Antenna Parameters

Future efforts could delve into more intricate optimization strategies for various antenna parameters, such as patch dimensions, substrate materials, and feed configurations. This would contribute to refining the antenna design for improved performance and efficiency.

### b) Beamforming and Beam steering Techniques

Exploration of advanced beamforming and beam steering techniques could enhance the antenna's ability to dynamically adapt to changing communication conditions. Implementing smart beamforming mechanisms could optimize signal directionality, coverage, and capacity in 5G networks.

### c) Integration of Advanced Materials

Investigating the integration of advanced materials, such as metamaterials or novel dielectrics, holds potential for further performance enhancements. These materials

could be tailored to manipulate electromagnetic properties, leading to improved antenna characteristics and overall 5G system efficiency.

**d) Performance Analysis in Realistic Scenarios**

Future research could involve conducting performance analyses in realistic and dynamic scenarios. Simulating the antenna's behavior in complex environments, including urban or densely populated areas, would provide insights into its real-world applicability and potential challenges.

**e) Integration with 5G Network Architectures**

The project's future works could explore deeper integration with evolving 5G network architectures. This includes investigating how the reflectarray antenna aligns with emerging communication standards, network densification strategies, and the deployment of small cells to optimize coverage and connectivity.

**f) Farfield Measurements**

Conducting extensive farfield measurements to validate and fine-tune the antenna's radiation characteristics. Real-world measurements would provide valuable data to compare against simulation results, ensuring the accuracy and reliability of the antenna's performance in practical applications.

## REFERENCES

- [1] Alsharif, M. H., & Nordin, R. (2017). Evolution towards fifth generation (5G) wireless networks: Current trends and challenges in the deployment of millimetre wave, massive MIMO, and small cells. *Telecommunication Systems*, 64(4), 617–637. <https://doi.org/10.1007/s11235-016-0195-x>
- [2] Chaharmir, M. R., Shaker, J., Gagnon, N., & Lee, D. (2010). Design of Broadband, Single Layer Dual-Band Large Reflectarray Using Multi Open Loop Elements. *IEEE Transactions on Antennas and Propagation*, 58(9), 2875–2883. <https://doi.org/10.1109/tap.2010.2052568>
- [3] Dahri, M. H., Jamaluddin, M. H., Seman, F. C., Abbasi, M. I., Ashyap, A. Y. I., Kamarudin, M. R., & Hayat, O. (2020). A Novel Asymmetric Patch Reflectarray Antenna with Ground Ring Slots for 5G Communication Systems. *Electronics*, 9(9), 1450. <https://doi.org/10.3390/electronics9091450>
- [4] Dahri, M. H., Abbasi, M. I., Jamaluddin, M. H., & Kamarudin, M. R. (2018). A Review of High Gain and High Efficiency Reflectarrays for 5G Communications. *IEEE Access*, 6, 5973–5985. <https://doi.org/10.1109/access.2017.2786862>
- [5] Attaran, M. (2021). The impact of 5G on the evolution of intelligent automation and industry digitization. *Journal of Ambient Intelligence and Humanized Computing*. <https://doi.org/10.1007/s12652-020-02521-x>
- [6] Costanzo, S., Venneri, F., Borgia, A., & Massa, G. D. (2020). Dual-Band Dual-Linear Polarization Reflectarray for mmWaves/5G Applications. *IEEE Access*, 8, 78183–78192. <https://doi.org/10.1109/access.2020.2989581>
- [7] Ali, M. M. M., & Sebak, A.-R. (2016). Design of compact millimeter wave massive MIMO dual-band (28/38 GHz) antenna array for future 5G communication systems.

- 2016 17th International Symposium on Antenna Technology and Applied Electromagnetics (ANTEM). <https://doi.org/10.1109/antem.2016.7550213>
- [8] Goudos, S. K., Antonios Tsiflikiotis, Babas, D. G., Siakavara, K., Christos Kalialakis, & Karagiannidis, G. K. (2017). Evolutionary design of a dual band E-shaped patch antenna for 5G mobile communications. <https://doi.org/10.1109/mocast.2017.7937640>
- [9] Bashir, S., M. Hashim Dahri, Shah, A., & Nasir, J. (2021). Design of a Wideband Reflectarray Element for Dual Band Operation in 5G Communications. <https://doi.org/10.1109/icet54505.2021.9689916>
- [10] Guo, Y. Q., Pan, Y. M., Zheng, S. Y., & Lu, K. (2021). A Singly-Fed Dual-Band Microstrip Antenna for Microwave and Millimeter-Wave Applications in 5G Wireless Communication. *IEEE Transactions on Vehicular Technology*, 70(6), 5419–5430. <https://doi.org/10.1109/tvt.2021.3070807>
- [11] Chou, H.-T., Wang, N. -N, Fang, M., Wang, L. -Q, Prayoot Akkaraekthalin, & Chou, H.-T. (2023). Dual-Band Reflectarray Antennas Using Integrated Resonant and Non-Resonant Natures of Metallic Waveguide Elements at Millimeter Wave Frequencies. *58(1)*. <https://doi.org/10.1029/2022rs007494>
- [12] Xia Xiaoyue, Wu, Q., Wang, H., Yu, C., & Hong, W. (2017). Wideband Millimeter-Wave Microstrip Reflectarray Using Dual-Resonance Unit Cells. *16*, 4–7. <https://doi.org/10.1109/lawp.2016.2551264>
- [13] Dahri, M. H., Jamaluddin, M. H., Khalily, M., Abbasi, M. I., Selvaraju, R., & Kamarudin, M. R. (2018). Polarization Diversity and Adaptive Beamsteering for 5G Reflectarrays: A Review. *IEEE Access*, 6, 19451–19464. <https://doi.org/10.1109/access.2018.2821358>

- [14] Rafique, U., Khalil, H., & Saif-Ur-Rehman. (2017). Dual-band microstrip patch antenna array for 5G mobile communications. 2017 Progress in Electromagnetics Research Symposium - Fall (PIERS - FALL). <https://doi.org/10.1109/piers-fall.2017.8293110>
- [15] Deckmyn, T., Maarten Cauwe, Dries Vande Ginste, Rogier, H., & Agneessens, S. (2019). Dual-Band (28,38) GHz Coupled Quarter-Mode Substrate-Integrated Waveguide Antenna Array for Next-Generation Wireless Systems. 67(4), 2405–2412. <https://doi.org/10.1109/tap.2019.2894325>
- [16] km5. (n.d.). CST Studio Suite 3DEM simulation and analysis software. Wwww.3ds.com. <https://www.3ds.com/products-services/simulia/products/cst-studio-suite/>
- [17] S-Parameters for Antennas (S11, S12, ...). (n.d.). [Wwww.antenna-theory.com](http://www.antenna-theory.com). Retrieved June 5, 2023, from <https://www.antenna-theory.com/definitions/sparameters.php#:~:text=In%20practice%2C%20the%20most%20commonly>
- [18] Antenna Theory - Near and Far Fields - Tutorialspoint. (n.d.). Wwww.tutorialspoint.com. [https://www.tutorialspoint.com/antenna\\_theory/antenna\\_theory\\_near\\_and\\_far\\_fields.htm](https://www.tutorialspoint.com/antenna_theory/antenna_theory_near_and_far_fields.htm)
- [19] “Microstrip Patch Antenna Calculator - Everything RF.” Everythingrf.com, 2019, [www.everythingrf.com/rf-calculators/microstrip-patch-antenna-calculator](http://www.everythingrf.com/rf-calculators/microstrip-patch-antenna-calculator).
- [20] Michael Kerner, Sean . “What Is 4G (Fourth-Generation Wireless)?” Search Mobile Computing, Apr. 2021, [www.techtarget.com/searchmobilecomputing/definition/4G](http://www.techtarget.com/searchmobilecomputing/definition/4G).

## APPENDICES

### Appendix A Gantt Chart For Final Year Project 1

ACTIVITY (FYP 1)	WEEK													
	1	2	3	4	5	6	7	8	9	10	11	12	13	14
Meet with supervisor														
Research literature review & gather information														
Submission of logbook progress														
Proposal writing														
Report writing														
Submission of draft report														
Submission of report														
Preparation for presentation														



## Appendix B Gantt Chart For Final Year Project 2

ACTIVITY (FYP 2)	WEEK													
	1	2	3	4	5	6	7	8	9	10	11	12	13	14
Meet with supervisor	█	█	█	█	█	█	█	█	█	█	█	█	█	█
Design and run the simulation using CST software	█	█	█	█	█	█	█	█	█	█	█	█		
Submission of logbook progress						█						█		
Troubleshoot the results									█	█	█	█		
Fabrication process											█	█		
Report writing										█	█	█	█	█
Submission of draft report													█	
Submission of Thesis														█
Preparation for presentation												█	█	█



## PSM2 Report Logha

### ORIGINALITY REPORT

**17%**

SIMILARITY INDEX

**11%**

INTERNET SOURCES

**14%**

PUBLICATIONS

**4%**

STUDENT PAPERS

### PRIMARY SOURCES

<b>1</b>	<b>www.scilit.net</b> Internet Source	<b>1%</b>
<b>2</b>	<b>www.researchgate.net</b> Internet Source	<b>1%</b>
<b>3</b>	<b>d197for5662m48.cloudfront.net</b> Internet Source	<b>1%</b>
<b>4</b>	<b>www.mdpi.com</b> Internet Source	<b>1%</b>
<b>5</b>	<b>Md. Sohel Rana, Sheikh Md. Rabiul Islam, Sifat Hossain, Md. Mostafizur Rahman.</b> "Design and Simulation of 2.45 GHz Microstrip Patch Antenna for S-Band Wireless Applications", 2023 14th International Conference on Computing Communication and Networking Technologies (ICCCNT), 2023 Publication	<b>1%</b>
<b>6</b>	<b>section.iaesonline.com</b> Internet Source	<b>1%</b>
<b>7</b>	<b>Xiaoyue Xia, Qi Wu, Haiming Wang, Chen Yu, Wei Hong. "Wideband Millimeter-Wave</b>	<b>&lt;1%</b>